

A CORRIDOR-BASED METHODOLOGY FOR THE DESIGN OF OPEN ACCESS  
HIGH OCCUPANCY TOLL LANE FACILITIES

A THESIS  
SUBMITTED TO THE FACULTY OF THE  
UNIVERSITY OF MINNESOTA  
BY

STEPHEN B ZITZOW-CHILDS

IN PARTIAL FULFILLMENT OF THE REQUIREMENTS  
FOR THE DEGREE OF  
MASTER OF SCIENCE

Adviser: JOHN HOURDOS

JANUARY 2017

© STEPHEN B ZITZOW-CHILDS 2017

## **ACKNOWLEDGEMENT**

I would like to thank Dr. Gary Davis and Dr. Greg Lindsey who graciously served on my committee despite the short notice and ever-changing schedule. I truly appreciate your flexibility and aid.

I would like to thank the Department of Civil, Environmental, and Geo-Engineering professors and staff for making my time at the University fun, engaging, rewarding, and fulfilling.

Most of all, I would like to thank my adviser and friend Dr. John Hourdos. In 2009, Dr. Hourdos took a chance on a third-year undergraduate new to the department. The opportunities he gave me to learn and grow, try and fail and pick myself up again helped me develop into who I am today. Even through the trials, I enjoyed every moment of my nearly seven years at the Minnesota Traffic Observatory. Thank you for seeing the potential in me and challenging me to attain it.

## **DEDICATION**

This thesis is dedicated to my loving wife Emma, without whom I would not have found the strength and determination to complete this project.

## ABSTRACT

Open access High Occupancy Toll (HOT) lane facilities allow vehicles to move freely into and out of the managed lane at any point along a corridor, permitting significant mobility from entrance and exit ramps. However, a potential safety concern exists when the mainline and HOT lanes are behaving differently. In certain circumstances, the general purpose lane adjacent to the HOT may be broken down while the HOT itself continues to operate at high speed (due to its managed nature). Vehicles seeking to enter the HOT must negotiate a potentially large (35 mile per hour or more) speed differential. As those vehicles enter the HOT, they must select a sufficiently large gap and accelerate to speed. Subsequent vehicles in the HOT may have to decelerate in order to avoid a collision, forming a shockwave in the HOT lane. This methodology models the formation of those shockwaves for varying conditions on the HOT and adjacent general purpose lane. Realistic traffic streams are reproduced for the HOT using measured parameters for headway and platoon formation and vehicles from the general purpose lane are introduced at varying low speeds. By iterating through this procedure many times, the distribution of shockwave lengths for any given conditions can be produced. The target conditions for modeling include 15 to 42 vehicles per mile on the HOT lane with vehicles being introduced with speeds between 10 and 45 miles per hour. These ranges were selected to cover conditions where the HOT has not broken down to a congested state while the general purpose lanes have. Analyzing historical data for a corridor allows the shockwave length distributions to be combined into comprehensive considerations of shockwave distributions for any given location within a corridor. Each of these comprehensive

shockwave distributions represents the overall behavior of the location over time. These can then be used to assess the safety of the corridor and provide guidance on regions within an HOT corridor which may require lane-changing prohibitions to improve safety.

# Table of Contents

Table of Tables .....	vi
Table of Figures .....	vii
Chapter 1 - Introduction.....	1
1.1 Literature Review.....	3
Chapter 2 - Shockwave Simulation.....	7
2.1 First-Estimate Traffic Reconstruction.....	13
2.2 Compacting the Stream.....	16
2.3 Perturbing the Stream .....	20
2.4 Introducing a Shockwave-Generating Disturbance .....	22
2.5 Shockwave Propagation.....	26
2.6 Shockwave Simulation Outcomes .....	28
Chapter 3 – Model Calibration .....	30
3.1 Calibration of Fundamental Traffic Parameters .....	32
3.2 Initial Calibration of the Car Following Model Parameters .....	37
3.3 Data for Calibrating and Validating Shockwave Distribution .....	39
3.4 Final Calibration and Validation.....	41
Chapter 4 - Characteristic Distributions .....	47
4.1 Building the Characteristic Distributions.....	48
4.2 Calibrated Characteristic Distributions.....	49
Chapter 5 - Assessing Historical Data .....	53
5.1 Density Increase Scenarios .....	61
5.2. Peak Periods Only Consideration .....	64
Chapter 6 - Corridor-Level Assessment Tool.....	66
6.1 Comprehensive Shockwave Distributions .....	68
6.2 Corridor Level Analysis.....	72
6.3 Assessment of I-35W in Minneapolis.....	75
Chapter 7 - Conclusion .....	88
References.....	92

## Table of Tables

Table 1. Vehicle parameters assigned at stream creation. ....	15
Table 2. Elements requiring calibration. ....	31
Table 3. Shockwave samples and their corresponding adjacent lane conditions. ....	40
Table 4. Calibration and validation results. ....	46
Table 5. Detector information for a portion of I-35W northbound in Minneapolis. ....	77
Table 6. Speed-Density region percentages by test scenario. ....	85



## Table of Figures

Figure 1. Important speed-density regions.....	8
Figure 2. Flow diagram for Stream Generation components of methodology. ....	11
Figure 3. Flow diagram for Shockwave Modeling components of methodology. ....	12
Figure 4. Density samples, from (top left) Stanitsas methodology 'base' condition, (top right) Stanitsas methodology 50% increased density scenario, (bottom left) this methodology's stream building, and (bottom right) this methodology after stream compaction to the 15 to 25 VPM region. ....	19
Figure 5. Distance and speed over time for the first 30 seconds (top left, top right) and the entire simulation horizon (bottom left, bottom right). ....	25
Figure 6. Speed versus density for Cliff Road HOT detector using all 2015 5-minute data. ....	33
Figure 7. Fitted two-piece speed-density relationship. ....	34
Figure 8. Fit of fundamental diagram for flow versus density. ....	36
Figure 9. Speed-density results from testing car following model parameters - example of a good fit. ....	38
Figure 10. Speed-density results from testing car following model parameters - example of a bad fit. ....	39
Figure 11. Cumulative distribution results for calibration using shockwaves in the 18 to 21 vpm density range. ....	45
Figure 12. Cumulative distribution results for validation using shockwaves in the 18 to 21 vpm density range. ....	45
Figure 13. Characteristic distributions based on the calibrated car following parameters. ....	50
Figure 14. Flow diagram for assessing historical data.....	56
Figure 15. Contour plot of historical data. ....	57
Figure 16. Convergence of historical data. ....	58
Figure 17. Heat map of historical data excluding weekends. ....	59
Figure 18. Convergence of historical data excluding weekends.....	59

Figure 19. Heat map of historical data within the characteristic distribution speed-density range.....	61
Figure 20. Increased density scenarios: 50% increase (top), 75% increase (middle), and 100% increase (bottom).....	63
Figure 21. Heat map of peak period only data for Cliff Road considering full ranges of speed and density (left) and only the characteristic distribution region (right). .....	64
Figure 22. Comparison of real data and Cliff Road fitted curve for location north of Highway 62.....	67
Figure 23. Comprehensive shockwave distribution for only Cliff Road. ....	69
Figure 24. Important speed-density regions.....	70
Figure 25. Surface rendering of comprehensive shockwave distribution.....	73
Figure 26. Comprehensive shockwave distribution using full day historical data. ....	74
Figure 27. Map of I-35W test corridor.....	76
Figure 28. Comprehensive shockwave distribution using full day data. ....	78
Figure 29. Comprehensive shockwave distribution using peak period only data.....	79
Figure 30. Proportion of speed-density regions for full day data. ....	80
Figure 31. Proportion of speed-density regions for peak period only data.....	80
Figure 32. Comprehensive shockwave distributions for 50% increase (top), 75% increase (middle), and 100% increase (bottom) scenarios, using full day (left) or peak period only (right) data. Note slight increase in lighter blues (greater number) of long shockwaves in higher increase scenarios as indicated by inset arrows.....	82
Figure 33. Proportion of speed-density regions for full day data under 50% increase scenario. ....	83
Figure 34. Proportion of speed-density regions for full day data under 75% increase scenario. ....	84
Figure 35. Proportion of speed-density regions for full day data under 100% increase scenario. ....	84
Figure 36. Proportion of speed-density regions for peak period data under 50% increase scenario. ....	85

Figure 37. Proportion of speed-density regions for peak period data under 75% increase scenario. ....	86
Figure 38. Proportion of speed-density regions for peak period data under 100% increase scenario. ....	86

## Chapter 1 - Introduction

Congestion during peak periods within major urban freeway networks is a perennial and chronic issue which plagues roadway managers worldwide. While many tools are available to help mitigate delays and reduce jams, High-Occupancy Toll (HOT) lane facilities have been an important component in dealing with severe congestion in Minneapolis, Minnesota. Two major freeways, with several more planned or under construction, include designated lanes which multi-occupant vehicles can use freely while single-occupant vehicles may opt to use the lane for a small, variable toll.

Although such facilities can be found in a wide variety of major metropolitan centers nationwide, design for the lanes has largely been left up to broad rules-of-thumb and engineering judgment. A strong framework for assessing the particular layout of a HOT lane facility has been lacking, from both a safety and a mobility perspective. Thus, a variety of approaches have been taken when implementing such infrastructure.

Two broad categories can be observed, which are referred to as open access and closed access facilities. Closed access facilities separate the HOT lane from the general purpose (GP) lanes, often simply using double white lines to prohibit lane changes along the majority of the lane. Vehicles may only enter or exit the lane at pre-specified 'gate' locations, which are generally located near major entrance or exit ramps to provide mobility for those using the HOT.

Alternatively, open access HOT lanes do not use gates and simply allow vehicles to move between the GP and HOT lanes freely. While this greatly increases mobility, since vehicles may access the HOT as quickly as they are able after entering the freeway and exit

the HOT as desired in order to reach any exit ramp throughout the corridor, there may be safety concerns with allowing lane changes at any point. These concerns stem from the key difference between the HOT and general purpose lanes within the corridor: the HOT lane is managed.

Since the HOT is controlled, albeit not strictly, by the tolling mechanism on the lane, the density on the HOT tends to remain notably lower than the adjacent general purpose lane and thus retain a higher prevailing speed. This is ultimately the goal of the HOT lane: to provide a higher level of service, and a more reliable journey, to those willing to pay. As a result, the disjoint in speeds between the HOT and adjacent GP lane can be quite significant. A properly managed HOT lane can continue operating at 50 MPH or higher while the mainline has broken down into a congested state. Thus, vehicles next to each other experience a speed differential on the order of 25 MPH or more! In such circumstances, vehicles attempting to traverse the lane boundary must negotiate the speed change and, in doing so, stand a high chance of causing vehicles to approach behind them and form a shockwave.

These shockwaves are the focus of this research effort. Shockwaves are a cause for concern since each approaching vehicle must make a braking maneuver in order to avoid a collision. In the HOT lane, where the prevailing speed is likely to be higher, this braking maneuver may be more severe and any increase in reaction time from distraction or error in speed estimation are potentially more liable to result in a crash.

The methodology which will be described in the coming chapters reconstructs traffic on the HOT lane for a variety of density conditions and models the generation of

shockwaves from vehicles entering the HOT and accelerating to the prevailing speed on the lane. By iterating through this methodology using a Monte Carlo sampling framework, the likely distribution of shockwave lengths which would propagate on the HOT lane can be developed for any arbitrary conditions which may arise on the roadway. In conjunction with an examination of historical data for a complete corridor, the Monte Carlo simulation tool can produce a unified assessment of shockwave generation throughout a region and map key areas which may require localized lane-change prohibitions (in the form of double-white striping or some other type of lane control).

This simulation structure is founded on data describing traffic patterns and shockwave generation along I-35W and I-394 in Minneapolis first used by Stanitsas (2014). The models used in this methodology are a notable improvement from those presented previously, in particular the General Motors (GM) car following model used for both validating the reconstructed stream to ensure realistic vehicle parameters and propagating shockwaves within the simulation procedure.

### 1.1 Literature Review

The concept of High Occupancy Toll lane facilities was developed in the early 1990s in response to underutilization of existing High Occupancy Vehicle lanes. Fielding and Klein observed in 1993: “Current HOV lanes are not very effective at reducing traffic; 43 percent of car-poolers are members of the same household. They cost everyone but serve few drivers.” To respond to this, they proposed charging a peak-hour toll to one- and two-occupant vehicles wishing to use the HOV lane. In the roughly two decades since, 11 states have implemented HOT lanes, covering 24 corridors (FHWA 2012).

As these HOT facilities have come online, they have been the focus of numerous studies. Many of these have concentrated on the pricing mechanisms used to operate the lanes. Lou, Yin, and Laval proposed a logit model which is calibrated using loop detector measurements and tolls over time in order to learn driver behavior and optimize the tolling rate (2010). Light (2012) performed a comprehensive examination of several tolling strategies across multiple corridor lane configurations. Total system travel time and toll revenue were calculated for algorithms seeking to (1) maximize revenue, (2) minimize total system travel time, and (3) maintain good HOT level of service. Also in 2012, Chung and Recker presented an evaluation methodology capable of optimizing for multiple policy targets. The methodology was demonstrated using a segment of SR-57 in southern California and showed effective pre-evaluation of a wide range of joint policies. Jang, Song, Choi and Kim proposed an algorithm for determining optimal tolls using a case study on the Gyungbu expressway in South Korea which improved lane use efficiency and shortened system travel time (2013). A mixed logit model was developed by Jang, Chung, and Yeo using a portion of I-680 in San Francisco as a case study. That study in 2014 involved both loop detector data and a traveler survey to determine usage and behavior. Another algorithm was proposed in 2014 by Zhang, Ma, and Wang which seeks to adapt toll rates based on a target flow rate in the HOT and detector data along both the HOT and GP lanes. The algorithm was experimentally tested within a VISSIM framework. Studies have also delved into operations questions surrounding HOT lanes. In 2009 Zhang, Yan, and Wang created a VISSIM-based HOT lane evaluation tool allowing practitioners to simulate various HOT tolling schemes to examine operational alternatives.

Research has also explored the motivation behind drivers using the HOT lane. In particular, Li in 2001 surveyed drivers using State Route 91 in California to determine what demographic and trip purpose factors are important in determining whether the HOT will be used. A simulation within TRANSIMS was developed to examine HOT lane user departure time, allowing individual drivers to adjust their trip to avoid high-toll times of day (Lee, Hobeika, Zhang, and Jung 2010). Along a similar track, Boyles, Garner, and Bar-Gera presented a framework for evaluating a HOT lane tolling algorithm which included departure time variability (2015).

Within the notable body of literature devoted to HOT lanes, only a small portion examines safety aspects directly. A recent work from the University of Florida for the Florida Department of Transportation used five years of fatal and injury crash data from facilities in California, Florida, Texas, and Washington to determine how HOT-related factors impacted crash occurrence (2015). The study concluded that the separation type and width between HOT and GP lanes can significantly impact crash frequency.

Numerous guidebooks at the state and federal level deal with HOT/express lane design. However, virtually all only consider designs which fall under the ‘closed-access’ approach. Washington State DOT’s *HOT Lane Buffer and Mid-Point Access* guidebook deals with connections between the HOT and GP lanes, but all other segments are assumed to be separated. Similar treatment is included within Florida DOT’s *Express Lanes Handbook 2015*, Nevada DOT’s *Managed Lanes and Ramp Metering Manual*, and the 2008 *Managed Lanes: A Primer* from the Federal Highway Administration (FHWA). Research into the design of weaving zones which are used within such facilities has been



done, including a paper from 201 by Yang, Mattingly, Williams, and Kim using a gap acceptance approach.

Open access design is only lightly treated whatsoever within the literature. A more recent effort by the FHWA, the *Priced Managed Lane Guide 2012*, includes information regarding the open access type facilities in Minnesota and elsewhere, but safety concerns in implementing such designs are not addressed. This research works to fill a portion of this gap, building extensively from the previous work completed by Stanitsas (2014) which developed preliminary methods for examining shockwave generation within the HOT lane due to lane weaving.

Within the methodology developed by this paper, a car following model is introduced. The car following model which was selected came from work done in the 1950s and 60s. Working from the General Motors laboratories in 1958, Chandler, Herman, and Montroll introduced a linear car following model which determines vehicle acceleration as a function of speed, relative speed between leader and follower, and spacing. That model was generalized a few years later to the model which is used in this effort – a non-linear version of the same underlying framework (Gazis, Herman, and Rothery 1961).

## Chapter 2 - Shockwave Simulation

Drivers which encounter a slower moving vehicle must decelerate in order to avoid a collision. Successively approaching vehicles are forced to slow as well, forming a shockwave. The response of each driver is an opportunity for an error – a misjudged speed or distance, a slowed reaction time to a change in behavior, etc. – which could lead to a collision. In the context of High Occupancy Toll lanes, this is of increased concern since the HOT is operated to maintain a high speed even when the mainline is congested and slow-moving. The purpose of this methodology is to estimate shockwave formation under a range of conditions in order to identify locations within HOT corridors which may require lane control to reduce the likelihood of crashes. Shockwave length is used a surrogate measure of safety, with longer shockwaves representing an increased risk of a collision for two reasons: more drivers must negotiate a deceleration and may make a mistake, and as a shockwave grows it is possible for the speed drop to become so severe as to make avoiding a collision impossible.

This approach examines a limited scope of conditions which are enumerated by the speed on the general purpose lane immediately adjacent to the HOT (simply referred to as the adjacent lane) and the density of traffic on the HOT lane itself. These two parameters were selected since the density on the HOT lane is the operative element which is used by the tolling algorithm to set prices on the lane and the speed on the adjacent lane is the speed at which a vehicle can enter the HOT lane. The range of conditions which will be considered can similarly be partitioned according to speed and density.

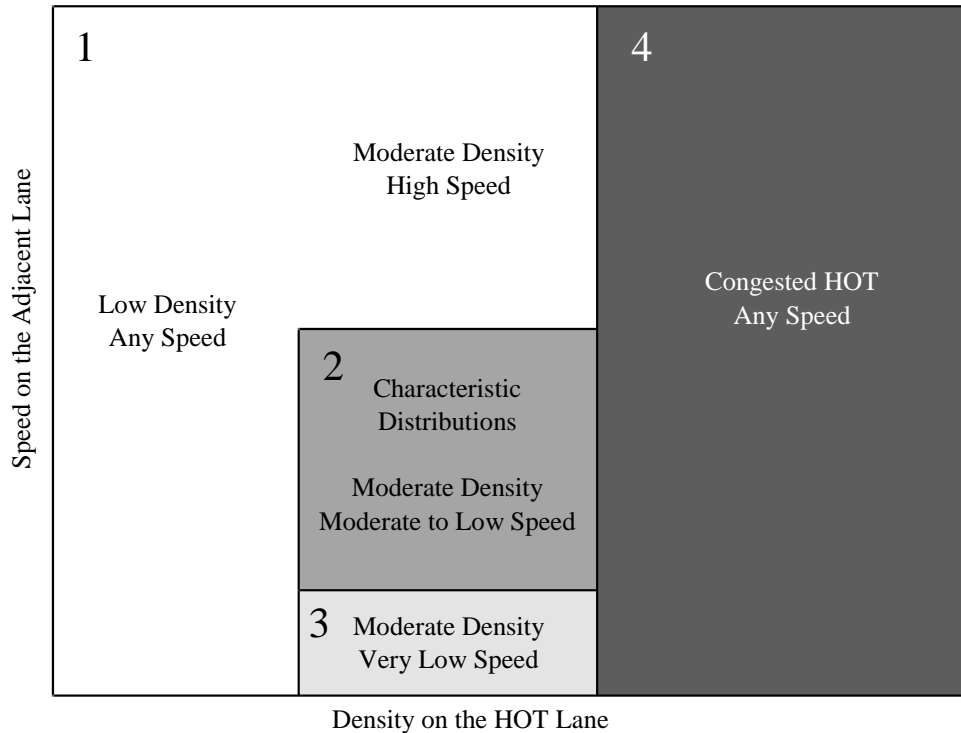


Figure 1. Important speed-density regions.

As Figure 1 shows, four major regions in speed and density can be enumerated. Region one, including low density on the HOT or modest density on the HOT while the mainline is at high speed, covers conditions where the risk of a shockwave forming are low. At low density on the HOT lane, vehicles are spread out with large headways between individual vehicles or small platoons (two to three vehicles clumped together). Any vehicle entering the HOT has a high probability of encountering a large gap, likely sufficient to even allow a vehicle accelerate from a complete stop to reach freeway speed without forcing any approaching vehicles to react. Alternatively, in the cases where the HOT lane has more closely space vehicles but the general purpose lanes are still moving along quickly, the speed drop between the two lanes is negligible so, although gaps are shorter in

the HOT, there is still enough room for vehicles to enter the HOT without causing a disturbance. Within region one, the assumption is made that no major shockwaves will form.

Region two is the core of this methodology and covers conditions where the adjacent lane has slowed sufficiently to become congested while the HOT continues to operate at uncongested densities. Within this region shockwaves are likely to form since vehicles entering the HOT lane are doing so at a lowered speed (possibly significantly lowered) compared to the HOT, which continues operating at roughly free flow speed, and the density on the HOT is high enough that large gaps are rarer and platoons in the HOT are longer and more frequent. At the upper and left-most edges of this region, shockwaves may be short or infrequent, but longer and more frequent shockwaves are likely to be found toward the lower right.

Region three is separated due to the severity of the speed drop between the two lanes. When the general purpose lanes are traveling at 10 miles per hour or lower, traffic is essentially stop-and-go conditions. If the HOT is still operating at uncongested speeds, the speed drop is in excess of 30 miles per hour. For this methodology, such conditions will be considered too severe for modeling.

Finally, region four includes all conditions where the HOT lane has broken down to a congested state. Under those circumstances, the speed on the HOT drops severely, and the speed differential between the HOT and adjacent lane decreases dramatically. Furthermore, the purpose of the HOT lane is to avoid congested conditions through the

pricing mechanism. Hence, congested conditions on the HOT will not be modeled. All of these regions will be revisited later when historical data is examined.

The methodology which will be presented here is founded on developing a stream of traffic which is representative of the HOT lane and introducing a vehicle to it at a lower speed to generate a shockwave. Doing so replicates the behavior of the HOT and adjacent general purpose lane at times and locations where vehicles attempt to enter the HOT, often bypassing significant congestion in the mainline. By repeating the shockwave generation methodology many times within a Monte Carlo sampling framework, a realistic shockwave distribution can be determined for any arbitrary pair of conditions on the two lanes of interest.

The overall structure of the methodology can be broken into several major components, which will be discussed in turn in the following sections: constructing a first-estimate traffic stream; validating the stream using the car following model; and introducing a disturbance and developing a shockwave. Ultimately, each of these components is until a stable sample of shockwave lengths is created for a wide variety of conditions. This chapter focuses on laying the groundwork for a single iteration through the shockwave simulation procedure, while the following chapter will extend the methodology to a corridor-based numerical approximation framework. Flow diagrams outlining the entire procedure are found in Figure 2 and Figure 3 below.

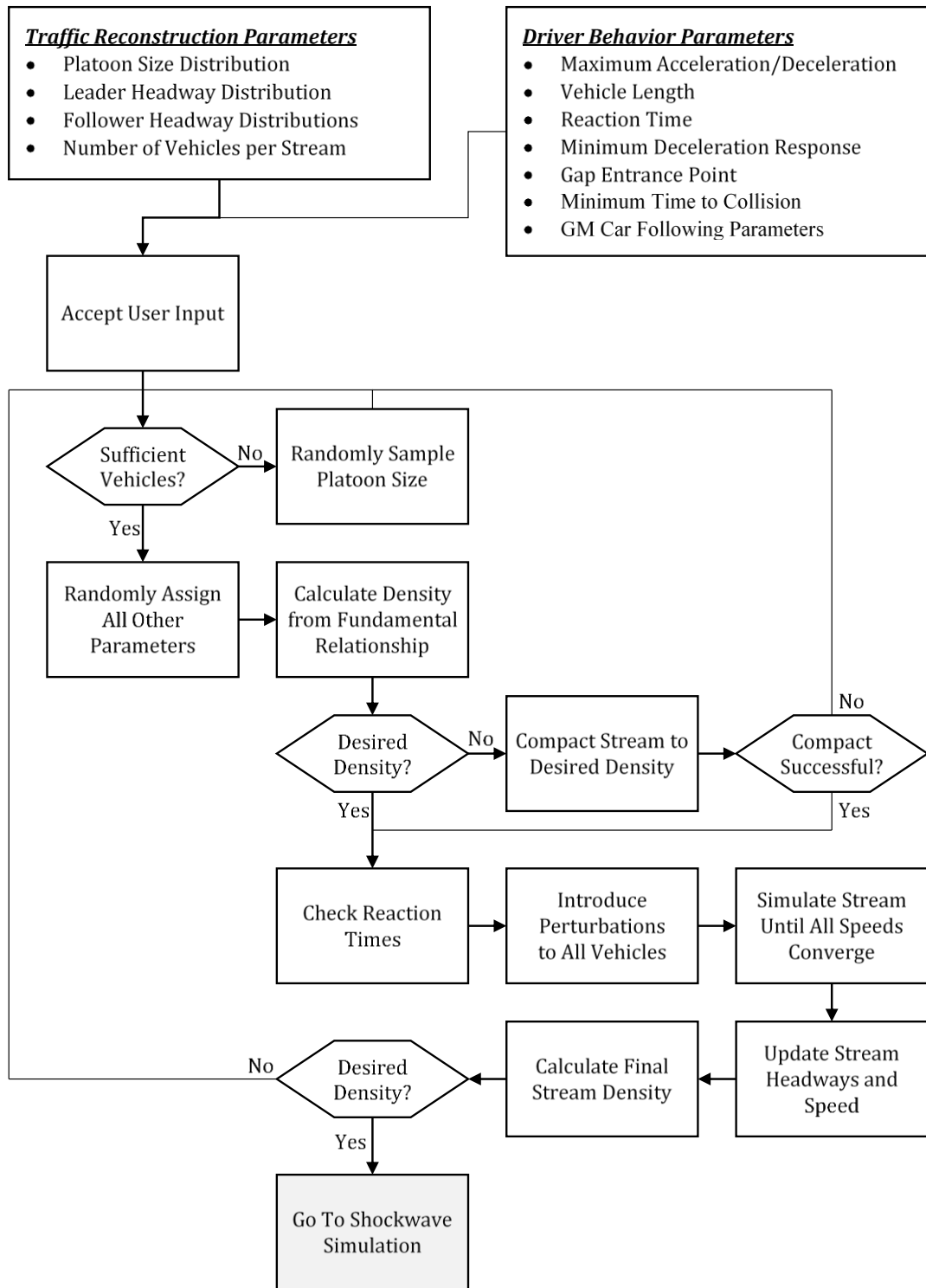


Figure 2. Flow diagram for Stream Generation components of methodology.

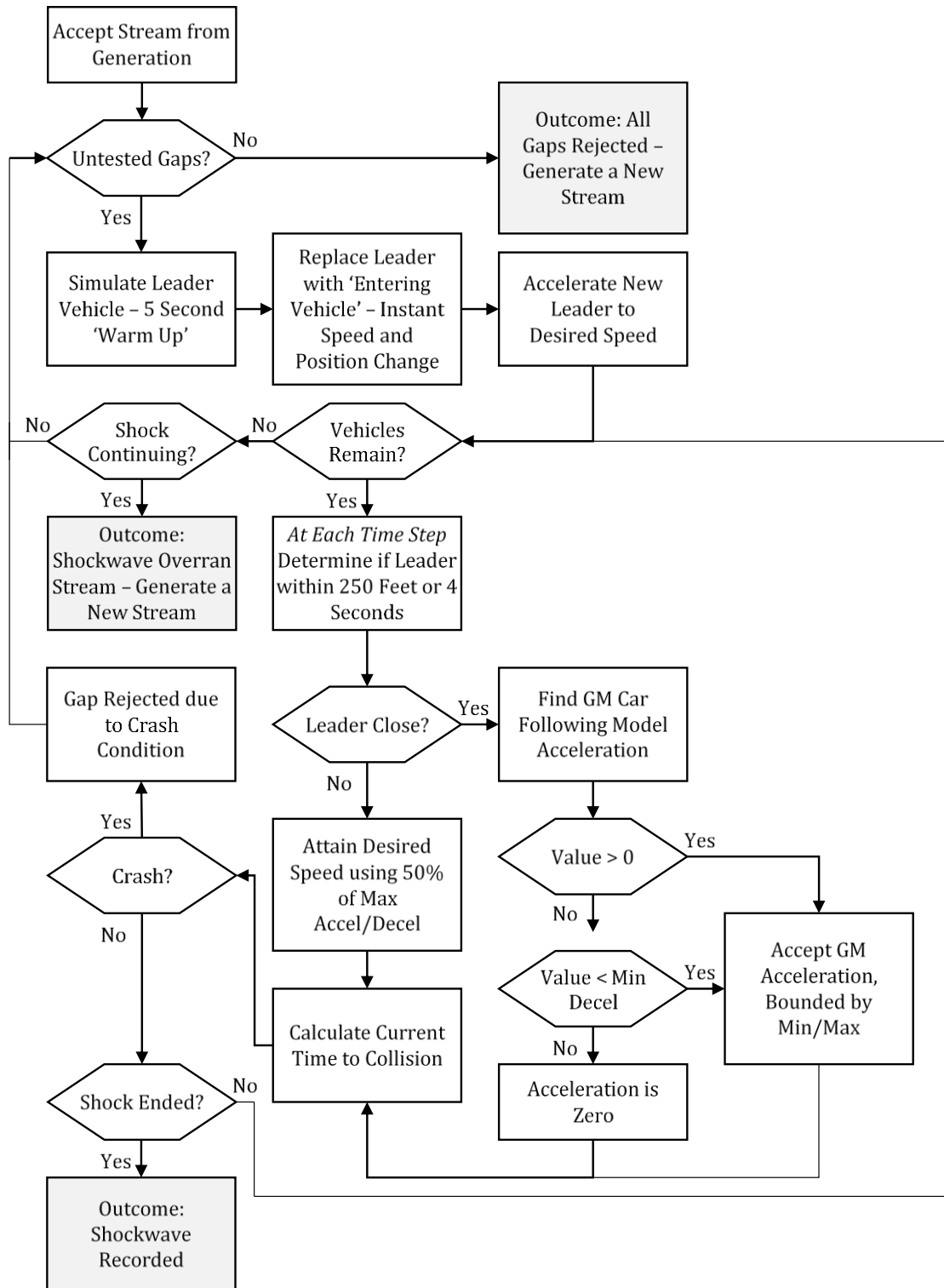


Figure 3. Flow diagram for Shockwave Modeling components of methodology.

From the figures above, after user input is set, a stream can be generated using a three-part structure including building a first-estimate reconstruction from static samples taken from real traffic, compacting the stream to a density within a desired range, and then modeling the stream using a fitted car following model to ensure a realistic traffic stream. Once that procedure is complete, shockwave simulation occurs (in Figure 3). Iteratively, gaps are selected for testing and a ‘new’ vehicle from the adjacent lane is inserted into the stream. Subsequent vehicles must then react based on the car following model acceleration response, and depending on the particular set of reactions three possible outcomes can be recorded: a successful shockwave of some measured length, every gap in the stream is rejected, or a shockwave propagates from some point within the stream until it reaches the final vehicle and does not dissipate (which is referred to here as a shockwave overrun).

### 2.1 First-Estimate Traffic Reconstruction

Building a realistic traffic stream with which to simulate shockwave generation is a fundamental building block of this methodology. Introducing shockwaves to a random collection of vehicles may produce an interesting distribution of responses, but the shockwaves thus created do not necessarily related to the behavior of any actual corridor. The particular parameters which describe the vehicles in this process must reproduce the same traffic patterns which are exhibited on the corridor of interest. To achieve this a two-fold approach was developed involving creating a best first-estimate traffic stream (which is itself completed in two parts, as will be described) and then allowing a GM car following model to validate the stream parameters and ensure that the stream is realistic for later simulation.



The first-estimate traffic stream is created by iteratively sampling values from three sets of data: platoon sizes, leader time-headways, and follower time-headways. For this research, data collected in Minneapolis by Stanitsas (2014) was used. Based on video recordings captured using overhead cameras at several gantries surrounding the Cliff Road portion of the I-35W corridor, platoons were identified using a two-piece approach developed by Benekohal, et al. (2004). This approach selects platoon leader vehicles based on either a 4-second time headway or a space headway of at least 250 feet. After identifying each leader, the remaining vehicles within each platoon were assigned a follower number based on their relative position within the platoon (i.e., first follower, second follower, etc.). For each position thus identified, including the platoon leader, time headways were collected and stored as individual vectors. Thus, all headways corresponding to platoon leaders were saved within a single vector, all headways corresponding to first-follower vehicles were saved within a separate vector, and so forth. As part of this enumeration, the length of each platoon was also recorded. Ultimately, only platoons of seven vehicles or fewer were kept for stream reconstruction, matching with the selection criteria used by Stanitsas (2014) included to remove rare outlier platoon lengths.

Since the eventual goal of stream creation is to simulate shockwave behavior, a large number of vehicles must be created so that sufficient space is available for the shockwave to propagate completely and dissipate. As will be described later, a stream of 500 vehicles is sufficient to encompass the majority of shockwaves, based on the conditions which were explored for this research. Using an iterative approach to reach the

desired stream length, platoons are created by sampling from the list of sample platoon sizes described above.

With a list of platoons, vehicles are implicitly created but lack any information regarding their spacing, speed, or behavioral characteristics. As a first approximation, headways are assigned randomly from the sets of measured headways described above. These headways give spacing to the reconstructed stream of vehicles, but several important parameters are still missing. These are listed in Table 1 and include characteristics which will be used within the overall car following procedure. Most of these characteristics are sampled from distributions described within traffic simulation literature, with one new parameter, the minimum deceleration response, introduced for this methodology.

*Table 1. Vehicle parameters assigned at stream creation.*

<b>Parameter</b>	<b>Units</b>	<b>Distribution</b>	<b>Mean</b>	<b>Sigma</b>	<b>Limits</b>	<b>Literature Source</b>
Maximum Acceleration	Ft/Sec <sup>2</sup>	Normal	5.6	1	-	Gipps, 1981
Maximum Deceleration	Ft/Sec <sup>2</sup>	-2x Acceleration	-	-	-	Gipps, 1981
Vehicle Length	Ft	Normal	18	2.25	-	Stanitsas, 2014
Reaction Time	Sec	Truncated Normal	1.01	0.37	(0.5, inf)	Johansson et al., 1971
Minimum Deceleration Response	Ft/Sec <sup>2</sup>	Truncated Normal	-1	0.2	(-inf, -0.5)	-

Acceleration and deceleration are assigned together, with vehicle acceleration drawn from a normal distribution and deceleration always assigned as twice the acceleration limit. Vehicle length is also taken from a normal distribution, and only accounts for passenger vehicles; no large vehicles are modeled. Reaction time is assigned from a truncated normal distribution, where the lower limit is set at 0.5 seconds to ensure

a reasonably long reaction time. In certain circumstances, a slightly shorter reaction time may be assigned at a later step in stream preparation; this will be described shortly.

The final parameter, minimum deceleration response, is a new parameter introduced by this methodology which limits the application of deceleration. The particular usage of the parameter will be discussed in detail when describing the car following model in a later section. Similar to reaction time, the minimum deceleration response parameter is selected from a truncated normal distribution, this time with a maximum value of  $-0.5$  feet/second<sup>2</sup>.

The streams reconstructed based from the platoon size and headway samples described above include some partial information regarding spacing and each vehicle is described by a set of useful characteristics, but the speed and density of the stream are as yet unknown. However, flow can be calculated since time headways are assigned and the total number of vehicles is known. Using flow and some relationship between the fundamental traffic parameters, speed and density are assigned. The particular relationship between these parameters is of great importance, and will be described in detail in the following chapter when the calibration of this framework is described. For this first step in stream generation, it is sufficient to know that the fundamental relationship is used to assign speed and density based on flow.

## 2.2 Compacting the Stream

After using the sampling techniques described above, a stream of vehicles with speeds, headways, and driver characteristics has been created. However, the ending density of this stream may not fall within a desirable range for simulation. As will be described further, at the corridor level a wide range of densities on the HOT must be simulated. Thus, a

methodology for altering – namely, increasing – the density of a generated stream is necessary.

Fortunately, a stream compacting methodology was already proposed by Stanitsas (2014). The reconstructed stream described above includes time headways which can be directly manipulated in order to increase the density of the stream. Based on the relationship between flow, speed, and density, a target density level can be transformed into a target total headway for the given stream of vehicles. Headway can then be incrementally reduced until the target headway is achieved or until no further headway reductions are possible.

The procedure developed by Stanitsas involves two main components. First, a flat percentage reduction of up to 10% is applied to every headway in the stream. If this is insufficient to meet the reduced headway total, a scoring mechanism is applied to the leader vehicle from every platoon. A score is assigned by the following equation:

$$Score = 5 * h_l - 2 * p_{l-1} \quad \text{Eq. 1}$$

Here,  $h_l$  is the headway of the leader vehicle  $l$ , and  $p_{l-1}$  is the platoon size associated with the leader ahead of the current leader vehicle  $l$ . After assessing the scores of every leader vehicle in the stream, the highest scoring leader is selected and has its individual headway reduced by 10%.

This headway shortening mechanism is limited by a minimum safe headway value of 2 seconds which must be maintained for each leader. If a leader would violate that minimum, its assigned score is reduced to zero. Once all vehicles in a stream have scores of zero, no further headway reduction can take place. If the stream has not met the required

density, the entire stream is thrown out and the reconstruction and compacting procedures are repeated until a stream with the desired properties is successfully generated.

Unlike the methodology developed by Stanitsas, the method for determining the target density was streamlined for this effort. Rather than calculating a particular percentage increase in density based on the starting density of the stream, the target density is selected directly using a uniform-random distribution covering a target density window. Thus, the actual stream densities in the target region are evenly distributed, rather than being heavily weighted toward the lower limit of each region.

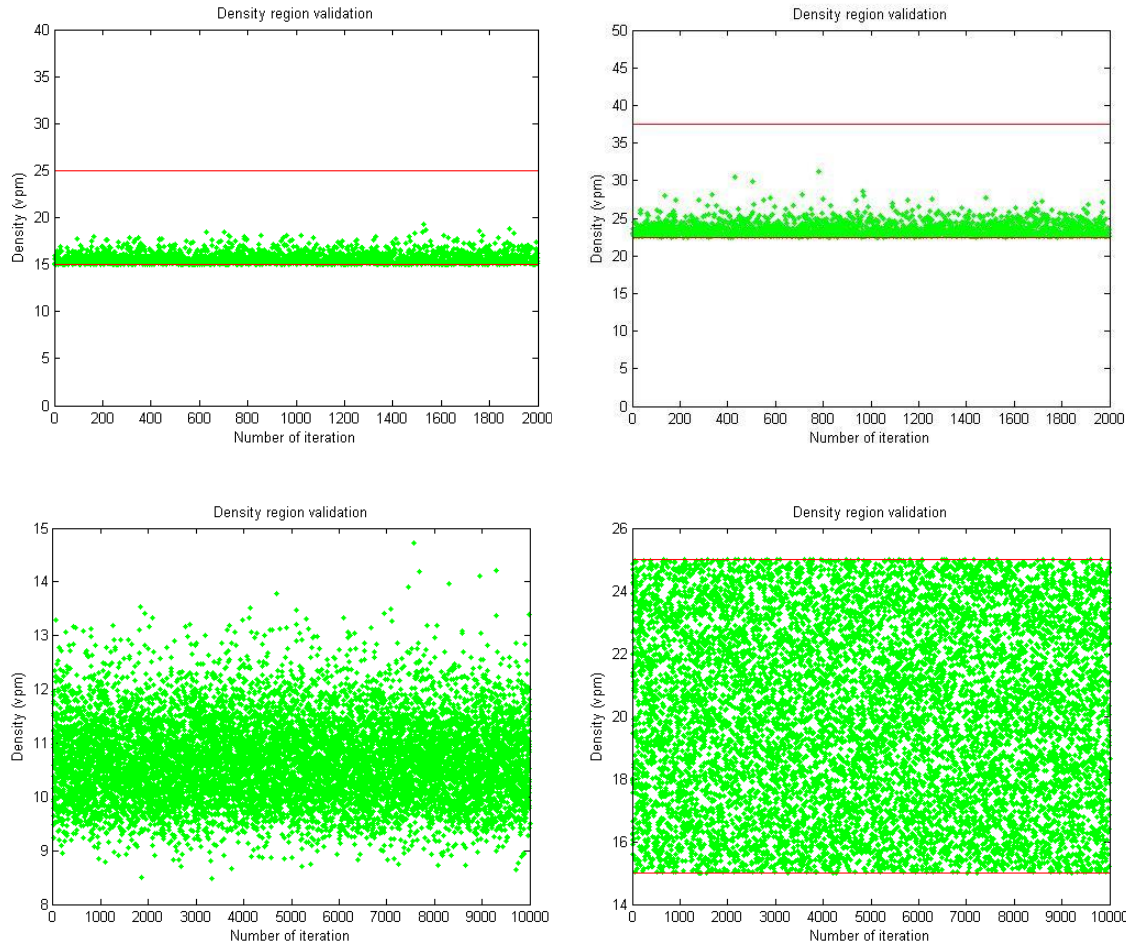


Figure 4. Density samples, from (top left) Stanitsas methodology 'base' condition, (top right) Stanitsas methodology 50% increased density scenario, (bottom left) this methodology's stream building, and (bottom right) this methodology after stream compaction to the 15 to 25 VPM region.

Figure 4 above illustrates this effect. The top two subfigures were taken directly from the Stanitsas paper, and show the starting density region samples and a particular density increase scenario. As can be seen, the reconstructed densities are strongly biased toward the lower limit of the 15 to 25 vpm region, with very few samples covering the region above 20 vpm. Scaling those samples upward results in a similar distribution stretched across a higher range. Alternatively, the bottom two subfigures show the method used in this paper. The densities taken directly after stream generation at the left are

generally found to be low (between 9 and 13 vpm). Randomly selecting a target density in an arbitrary region (for example 15 to 25 vpm, as shown in the lower right) produces a well-balanced set of densities across the desired range.

### 2.3 Perturbing the Stream

The streams created from samples, assigned randomized characteristics, and compacted to the desired final density range represent a good first estimate for simulation but lack internal agreement between parameters. In order to ensure that the stream is realistic, the relationship between the assigned headways and speeds must be checked by allowing a car following model to interact with the stream and find a convergence. A methodology was developed to introduce perturbations throughout the stream to prime the GM car following model and force each vehicle to negotiate a desired headway.

Prior to perturbing the stream and running a simulation, consistency between the headways within the stream and each vehicle's given reaction time must be checked. Within the random framework described for stream building, it is possible for vehicles to have assigned headways which are extremely short relative to their reaction time. This does not represent a realistic situation – drivers with poor reaction time tend to follow at larger headways to account for their poor ability to respond to change. Thus, a correction was introduced to provide some minimal correspondence between following time and reaction time. Any vehicle having a reaction time greater than 175% of its following headway has its reaction time reduced to meet that criterion. This value of 175% was found through experimentation with the stream perturbation methodology and was selected based on the ability of the perturbed stream to converge safely without vehicles failing to respond in time due to inadequate initial headways.

With a correspondence established between headway and reaction time, the stream is more realistic, but the selected headways for each vehicle are still artificially selected from static distributions and do not correspond to the behavior of each vehicle. Thus, simulating the entire stream in order to establish those relationships is necessary. The first vehicle in the stream initializes a simulation environment for the remainder of the stream. This leader is placed at an arbitrary distance (during development of this methodology this was set at 1000 feet from the origin) and assigned the target speed of the stream (as selected from the fundamental diagram relationship and the target density). The first vehicle retains that speed throughout and does not interact with the GM car following model whatsoever. Since no vehicle precedes it, the first vehicle serves only to set the leading edge of the simulation space.

Every subsequent vehicle is assigned two speeds for use in simulation. First is the same target speed as the first vehicle – that is, the target speed for the entire stream from the fundamental diagram. The second is an initial ‘perturbed’ speed which is selected from a random normal distribution centered on the target speed for the stream. This introduces the necessary stochastic element to trigger the GM car following model. Only slight speed differences are required to prime the GM model, so the normal distribution sigma was set at 2 feet per second.

For the first time step for every vehicle, their starting location is calculated using the perturbed speed which they were assigned and the headway which they retained from the stream creation/compacting process. Following the first time step, every vehicle uses their reaction time and the GM car following model to select an acceleration at every 0.1



second time step. Each vehicle only observes the vehicle directly in front. In such cases where sufficient time has not elapsed at the beginning of the simulation for reaction time to be used, no acceleration is implemented and simple kinematics are used to move the vehicle forward one time step. The process repeats until all vehicles reach the desired speed for the stream within a set tolerance (in this methodology, within 0.1 foot/second), or terminates if vehicles overlap and ‘crash’ (in which case the stream is rejected and regenerated).

Once converged, the simulation results are used to update the headway and speed parameters of the first-estimate stream. Each vehicle’s time headway is calculated using the final spacing and the desired speed of the stream and replaces the original headway which was assigned by random sampling. The desired speed for each vehicle is then set uniformly to the previously used target speed. The density of the final stream is then checked to ensure that it conforms to the desired density window introduced at the beginning of stream generation. If the stream conforms, it is ready for use with simulation and represents a realistic set of vehicles. Again, a non-conforming stream is rejected and regenerated until a satisfactory stream is created.

#### 2.4 Introducing a Shockwave-Generating Disturbance

By randomly selecting parameters for a stream of vehicles and then simulating that stream to allow a natural convergence, a realistic traffic stream is achieved which is representative of the HOT lane. Modeling shockwaves using streams generated by this methodology can then provide meaningful information regarding the behavior of a HOT lane facility. The mechanism for introducing disturbances to produce such shockwaves is the focus of this section.

The time headways which are coded into the traffic stream represent gaps that a vehicle from the general purpose lane may attempt to enter and occupy. In this shockwave simulation methodology, instead of using a gap selection model to probabilistically choose which gap to accept, each gap is examined in turn and a potential shockwave is introduced. If that shockwave completes successfully, the gap is ‘selected’ and the shockwave is recorded. If a ‘crash’ condition would occur, as will be described in the next section, the gap is rejected and the next gap is tested, repeating until a satisfactory gap is located.

For any given gap tested the disturbance is created by simulating a vehicle entering the HOT lane from the adjacent lane. This is governed by two parts: the location within the gap where the vehicle attempts to enter, and the speed at which the new vehicle merges. The location within the gap is selected from a random distribution which is bounded by high and low limits. The mean and sigma of this random distribution were part of calibration which will be described in detail in the following chapter. The maximum and minimum values were forced to 5% and 80% of the gap length, and were not explicitly calibrated. Rather, these two values were meant to achieve realism with regard to the lane changing vehicle’s behavior. In the case of the 5% limit, vehicles moving from the general purpose lane to the HOT lane require some transition time between lanes and drivers will only begin moving into the available gap once the vehicle at the front of the gap has passed. The 80% limit removes cases where vehicles move into the HOT immediately in front of a fast-moving vehicle and immediately cause a simulated crash – although not strictly necessary since the simulation methodology would capture such behavior by rejecting the gap, this does eliminate essentially unreasonable gap selection behavior from simulation.

After selecting a location within the gap, the speed of the 'new' vehicle is required. This is taken from a random uniform distribution based on the desired range of speeds for the adjacent lane.

The actual introduction of the entering vehicle is done by instantaneously modifying the location and speed of the first vehicle in the stream to that of the new vehicle. After a short period of warmup (5 seconds) in which the lead vehicle (in the HOT) travels at the prevailing speed of the HOT, the leader is stepped forward as normal for one time step (0.1 second) and then moved backward according to the portion of the trailing gap which corresponds to the random gap entrance point described above. Thus, for a leader traveling at 60 feet per second, with a trailing gap of 1000 feet, and a gap entrance percentage of 30% selected, the vehicle moves forward 6 feet (0.1 second at the given speed) and then is moved backward by 300 feet (30% of the trailing gap) to the new position of the vehicle entering from the general purpose lane. After moving backward, the leader's speed is modified to match the random adjacent lane speed sample. From there, the 'new' vehicle accelerates as quickly as possible to reach the prevailing speed of the HOT lane. Figure 5 below illustrates this methodology. Note that since the behavior of the original leader becomes irrelevant to the simulation of the shockwave after the new vehicle is inserted into the stream, that original leader is no longer simulated.

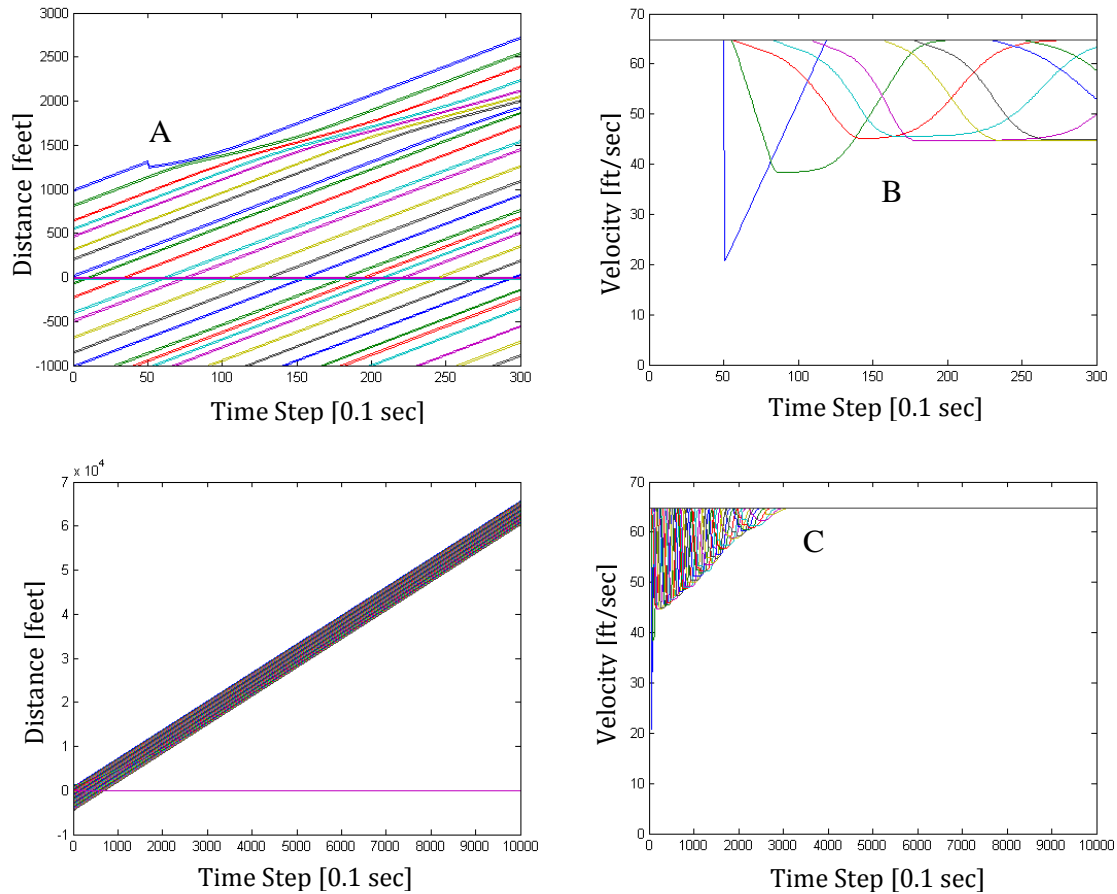


Figure 5. Distance and speed over time for the first 30 seconds (top left, top right) and the entire simulation horizon (bottom left, bottom right).

As can be seen in Figure 5, the first vehicle is replaced and starts a shockwave at indication A. Subsequent vehicles are then forced to respond by slowing and then returning to speed once they are able. At indication B we note that several vehicles are forced to make almost identical decelerations from desired speed, showing that for this condition the shockwave was continuing without significant change in intensity. However, over the long run, as shown at indication C, the shockwave subsided with significant space left over within the simulation horizon.

## 2.5 Shockwave Propagation

After the first vehicle's trajectory is established, all subsequent vehicles in the stream are modeled using a car following model. For this methodology, a General Motors car following model was incorporated in a two-component framework. Prior to assigning an acceleration to a vehicle, the time and space headways between the vehicle and its leader are found. If the leader is further away than either 250 feet or 4 seconds (the same limitations which were used to identify platoon leaders, based on Benekohal, et al. 2004), the current vehicle accelerates or decelerates to reach desired speed, i.e. the prevailing speed of the HOT. If the leader is within one or both of those boundaries, the GM model acceleration response of a given vehicle is determined by the following equation:

$$accel = \frac{\alpha * v_i^M}{(x_{i-1} - x_i)^L} * (v_{i-1} - v_i) \quad \text{Eq. 2}$$

The acceleration response is proportional to both the speed differential between the current vehicle and its leader and the speed of the current vehicle, with the current speed being raised to some power M. The acceleration response is inversely proportional to the distance between the current vehicle and its leader, with this term being raised to some power L. The entire acceleration response is also modified by a sensitivity coefficient, alpha. The particular values of each of these parameters will be discussed in the following chapter.

At every time step, with reaction time accounted for, the GM model acceleration response is calculated, and one of three actions is taken:

1. If the acceleration is greater than zero, the acceleration is accepted, so long as it falls under the maximum limit specified for the vehicle (which

was assigned during stream generation). Otherwise, the maximum acceleration of the vehicle is used.

2. If the recommended acceleration is less than zero, two alternatives are examined. For very weak deceleration responses, no actual acceleration will be applied. In this case 'very weak' means a value between the minimum deceleration response parameter, which was assigned at stream generation, and zero.
3. In the second alternative, which includes stronger decelerations, the GM given acceleration response is again accepted, so long as it does not violate the maximum deceleration (twice the magnitude of the vehicle's maximum acceleration).

Once a course of action has been selected and the acceleration rate is finalized, simple kinematics convert the acceleration to an updated velocity and position after one time step. Following this update, the time to collision for the current vehicle is calculated based on the available gap and speed. If this value falls too low, and the current vehicle approaches its leader too closely, a 'crash' condition occurs and the shockwave fails. Note that this distance includes some buffer distance between a vehicle and its leader; vehicles do not need to physically overlap for a 'crash' condition to occur. Two values for this time to collision limit were incorporated into the model: one which only applies to the first vehicle after the entering vehicle, and one for all other vehicles in the stream. Since the entering vehicle is actively assessing gaps in the HOT lane and is not already accustomed to traveling within that stream, it is possible that they have a different behavior pattern in

terms of the minimum trailing gap which they will allow. Vehicles already in the HOT stream and traveling at a higher speed may respond differently than the entering vehicle. E.g., the new vehicle may reject a gap if a vehicle would approach within 60 feet of them from the rear, whereas subsequent vehicles in the shockwave may tolerate vehicles approaching within 30 feet before a crash condition is triggered. These two parameters will be discussed again during calibration.

## 2.6 Shockwave Simulation Outcomes

The flow diagrams shown above indicate three possible outcomes of simulation: either a shockwave propagates successfully and is recorded as having some length, or the simulation fails either due to a “shockwave overran stream” condition or an “all gaps rejected” condition. In the shockwave overran stream case, a shockwave was formed and propagated until the entire set of vehicles available within the stream were forced to maneuver. Thus, the last available vehicle became involved in the shockwave and the shockwave did not dissipate. Since this methodology does not introduce a mechanism for dynamically adding vehicles to the stream, the stream is deemed insufficient and is rejected, forcing a new stream generation and shockwave simulation cycle.

Similarly, a new cycle occurs if the all gaps rejected condition is met. In this case, each gap within the stream is successively examined and a crash condition is generated for every gap. Thus none of the available gaps within the stream is found to be suitable. As with the previous case, a method for dynamically adding vehicles to the stream in order to provide more available gaps is not included and the simulation procedure must terminate. A new stream is generated and fresh attempts are made to create a successful shockwave.

Both of the conditions given above are theoretically possible within traffic under certain consideration constraints. Although a shockwave cannot build forever, as in the first case, if only a segment of traffic is considered, every vehicle could be involved in a shockwave. Similarly, a vehicle in the general purpose lane could spend an extended period of time examining and rejecting gaps within the HOT, ultimately not finding one for minutes or abandoning the effort altogether. However, the simulation space within this research included 500 vehicles on the HOT lane. With such a large number of opportunities for lane changing and such a large set of vehicles in which to propagate, the possibility of either of these two cases occurring is extremely small. Thus, when they occur, they are treated as outlier conditions and rejected. This also becomes of utmost importance when combining methodologies for a corridor-wide assessment later, as will be described.



## Chapter 3 – Model Calibration

The methodology presented in the previous chapter has many parameters encapsulated within it which require some level of calibration in order to match simulation results to local conditions. One such component, the relationship between fundamental diagram parameters, has already been explored, but must be revisited. Beyond this, the car following model and driver behavioral parameters which were input also require some attention.

A detailed examination of the source of the shockwave data used for calibration and validation is also of key importance. The particular assumptions underlying the data directly influence and constrain the methodologies which can be used for calibration. Ultimately, the results of calibration and validation for this analysis will be presented, and a discussion regarding the effectiveness of the calibration in certain circumstances will follow.

The elements which are calibrated in the following sections rely upon certain data sets which change under different sets of circumstances. Certain pieces of information change on a location-by-location basis within a corridor, while other parameters only change infrequently. The calibrations performed on the methodology itself to ensure that the mechanisms inherent to the process are reasonable must only be done rarely when those assumptions are challenged or when the methodology is applied to situations which are wholly different from those presented in this research. These elements are indicated in Table 2:

*Table 2. Elements requiring calibration.*

<b>Element</b>	<b>Frequency of Calibration</b>
Fundamental Diagram Relationship	Per Location
Traffic Reconstruction	Infrequently/Per Corridor
Driver Behavior	Infrequently/Per Corridor
Car Following Model	Rarely/Significant Change
Shockwave Formation	Rarely/Significant Change

The methodologies developed in Chapter 2 compose the foundation for a tool which will be elaborated upon in later chapters. When using the tool, the more localized elements are calibrated frequently to conform to target areas as identified by traffic managers. The fundamental diagram relationship between speed, density, and flow falls within this category. Varying locations within a corridor could have notably different fundamental relationships. Recalibrating that component of the model is required whenever the fundamental diagram changes significantly.

Stepping out from the localized behavior of the fundamental diagram, traffic reconstruction and some driver behavior parameters are generally stable across entire corridors or throughout a region. Platoon formation patterns, traffic composition, and vehicle performance characteristics are presumed to be stable across a corridor since the population of drivers is consistent. Moving to a different corridor or applying the methodology to a different region within the world would necessitate a recalibration of these parameters. i.e., certain driver and vehicle characteristics in Minneapolis may differ from those in Chicago, San Diego, or Atlanta.

Finally, the overall methodology was calibrated using high resolution information regarding shockwave formation and, thus, car following. The GM model and shockwave propagation mechanisms which are discussed in the final section of this chapter must only

change when driver behavior is expected to vary significantly from the calibration conditions. Recalibrating these components would require similar high resolution data for the new condition, and each of the other sub-components in the methodology would be affected.

### 3.1 Calibration of Fundamental Traffic Parameters

At several points throughout the simulation methodology laid out in the previous chapter, the relationship between speed, density, and flow is referenced. This fundamental relationship is well used within traffic simulation, and a wide variety of models have been developed to relate the three parameters. For this methodology, an examination of data for the HOT lane detector at Cliff Road was completed in order to establish a fitted relationship by which to tie the simulation results to the real world.

The fitting procedure incorporated all 5-minute aggregated traffic measurements from the loop detector at Cliff Road during 2015, totaling some 105,120 individual measurements. Since the detector is a single loop, speed is estimated from volume and occupancy using a calibrated field length. Of the measurements which were collected, any empty or error-flagged values were removed, leaving 50,028 good measurements. Further, data points with speeds over 80 mph or densities under 3 vpm were excluded from the fitting process to avoid errors in estimation which occur when volumes are extremely low. From the remaining data, a two-piece fitting procedure was implemented which features a flat value of speed for low densities, and a polynomial fit between speed and density for higher density ranges. Figure 6 below shows the data which was collected.

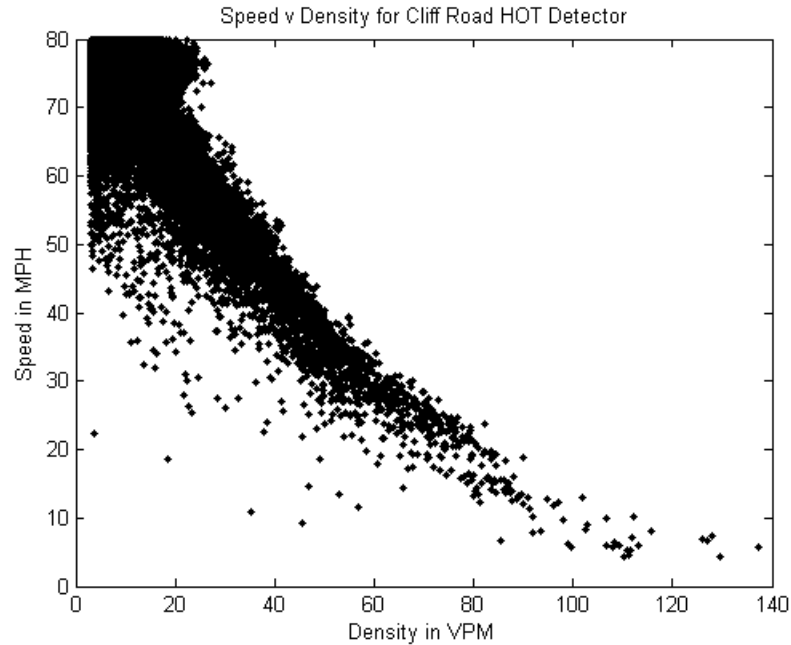


Figure 6. Speed versus density for Cliff Road HOT detector using all 2015 5-minute data.

Based on the data in the figure, a jam density value of 140 was estimated visually. Using this value, the polynomial fit was evaluated by minimizing the following equation:

$$\min \sum (v_i - \beta(k_i - 140)^2)^2 \quad \text{Eq. 3}$$

This minimization is the sum of squared differences between the data pictured above and a 2nd order polynomial with both roots at 140 vpm and controlled by the coefficient  $\beta$ . This minimization was also subject to a limit such that only data above a specified density threshold was considered. Below this threshold, speed was held constant at the same value as the edge of the polynomial, thus forming a continuous function with a single sharp disjoint at the threshold.

By manually adjusting the threshold and allowing the minimization function to select the  $\beta$  parameter, a fitted curve was found, and is described in Figure 7 below. Rather

than simply showing the point cloud against the fitted curve, Figure 7 shows a boxplot for every 1-vpm segment of the data (i.e., all data between 3 and 4 vpm forms a boxplot, all data between 4 and 5 vpm forms a boxplot, and so forth). This visually clarifies the density of the point cloud while still representing the full spread of data. For each boxplot, the box bounds are at the 25th and 75th percentiles of the relevant data, and the whiskers extend to the 5th and 95th percentiles.

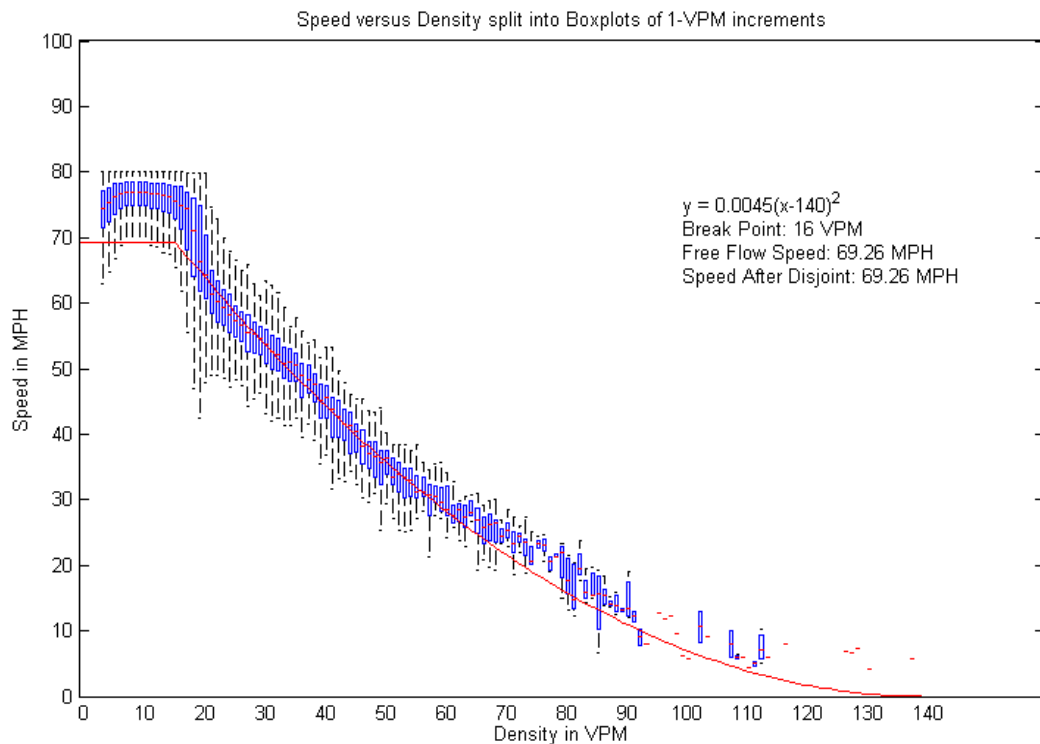


Figure 7. Fitted two-piece speed-density relationship.

As indicated in the figure, the  $\beta$  parameter was set to 0.0045 and the breakpoint between the polynomial fit and the uniform speed was selected as 16 vpm. The speed at 16 vpm was controlled by the polynomial fit, setting it to 69.26 mph. This value was then kept for all lower densities, despite being notably below the mean values, which hovered near 76 or 77 mph. The speed limit of the roadway is 55 mph at this location, so a low-

density free flow speed of roughly 70 mph was deemed an adequate compromise between the posted conditions of the roadway and the actual data at low densities, and furthermore allows the two-piece fit to remain continuous which eliminates any unusual behavior from a sudden change in speed at the transition point. The fit across 15 to 42 vpm is of primary importance since that region covers the conditions which will be modeled. Within that range, the fit falls close to the mean of observed data, barring a small area at roughly 35 vpm where the fit still falls within the middle 50% of data (the blue region in the figure).

The fit was then translated into a similar curve for flow versus density. Rather than developing an analytic solution, which involves a complex solution to a cubic function, a numerical approach was taken, with the fine-grained resolution of 0.1 vpm to ensure accuracy between flow and density.

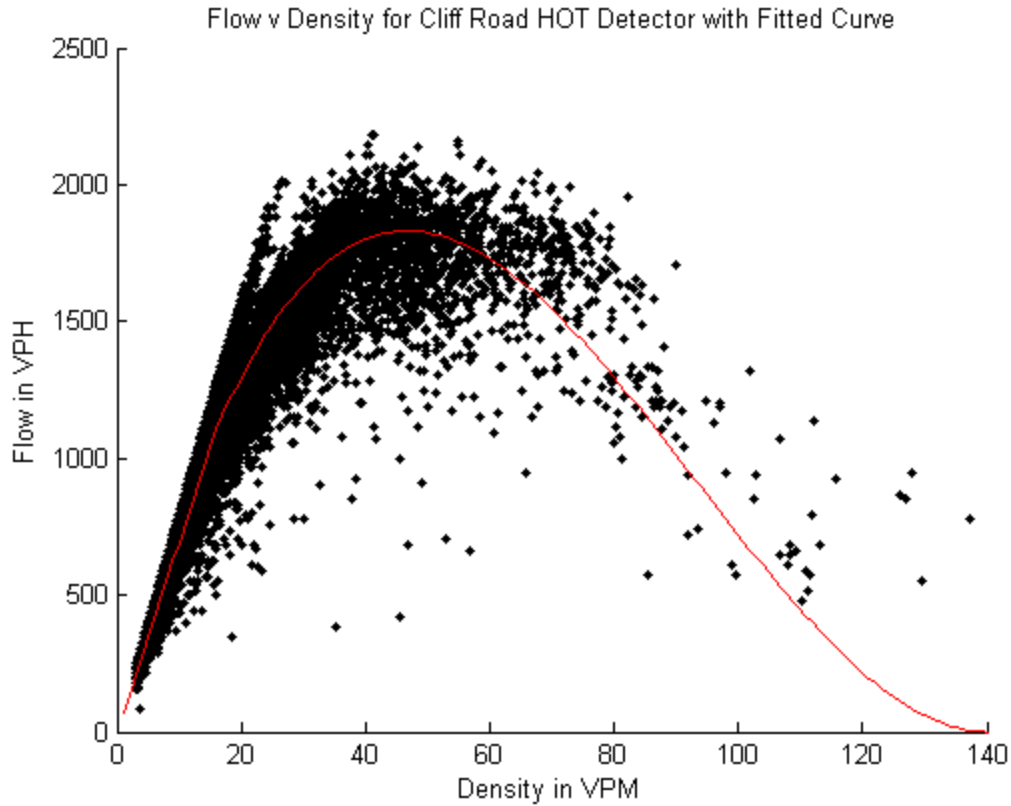


Figure 8. Fit of fundamental diagram for flow versus density.

As can be seen from the fitted curve in Figure 8, the linear portion of the fit at low density tracks slightly underneath the high edge free flow speed. This corresponds with the roughly 9 mph difference between observed free flow speeds and the set free flow speed for the two-piece fit. The 3rd order curve reaches a reasonable although slightly low capacity value near 1800 vph. For the range of values which will be dealt with throughout the remainder of this analysis, 15 to 42 vpm, flow corresponds one-to-one with density, so no special consideration need be made for higher densities (at lower speed) which result in the same flow as lower densities (at higher speed).

### 3.2 Initial Calibration of the Car Following Model Parameters

With the fundamental diagram data from the previous section, it becomes possible to examine sets of car following model calibration parameters. This is done by generating a set of speed-density data points using the stream perturbation methodology described previously and comparing the results against the fitted fundamental diagram to ensure a good fit. Car following model parameter sets which produce unreasonable speed-density curves are discarded. For reference within this section, the GM car following equation is reproduced below.

$$accel = \frac{\alpha * v_i^M}{(x_{i-1} - x_i)^L} * (v_{i-1} - v_i) \quad \text{Eq. 4}$$

To ensure comparability of results, a set of 540 streams were pre-generated and stored for repeated simulation. 20 streams were generated for every 1-vpm within the range 15 to 42 vpm (i.e., 20 streams with densities between 15 and 16 vpm, 20 streams between 16 and 17 vpm, etc.). Using these streams, and varying sets of GM model parameters, stream perturbations were introduced and simulated until convergence. The resulting final stream speed-density pairs were used to compare with the fundamental diagram relationship established above. If the simulated values agreed with the fundamental diagram, the car following model parameters were deemed acceptable. Non-conforming speed-density distributions resulted in car following model parameter sets being discarded as unrealistic.

Within the perturbation regime described above, a limit is also imposed: if simulation of the stream perturbations would cause vehicles to overlap one another, i.e. crash, the simulation is rejected, and if this rejection occurs many times (more than 30) for



any given stream, further attempts to simulate are not made. In this way, bad combinations of car following model parameters are also rejected. This is demonstrated in Figure 9 and Figure 10 below, which show a well-calibrated car following model parameter set and a poorly-calibrated car following model parameter set, respectively.

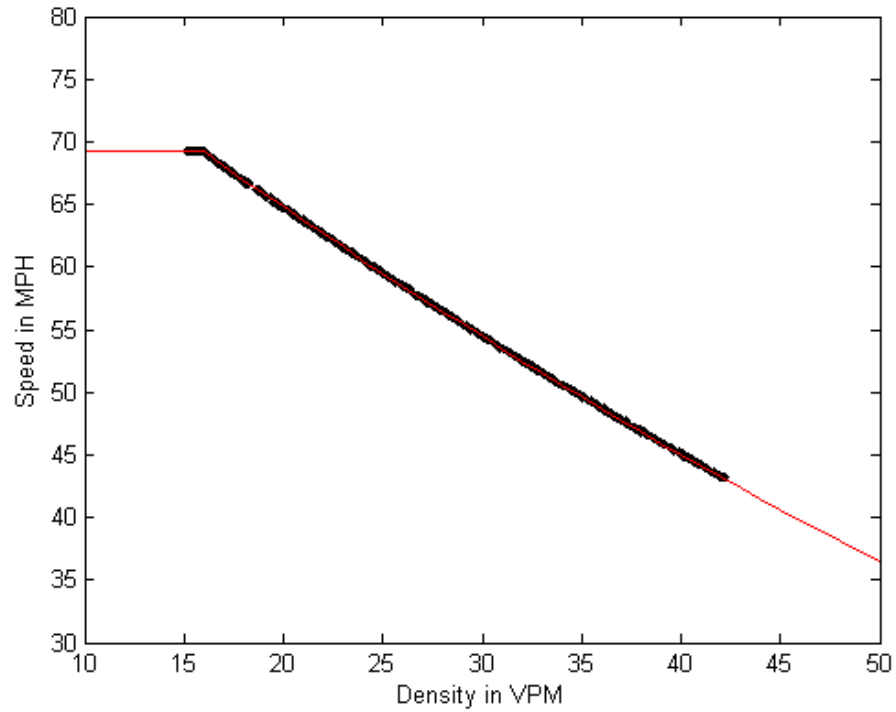


*Figure 9. Speed-density results from testing car following model parameters - example of a good fit.*

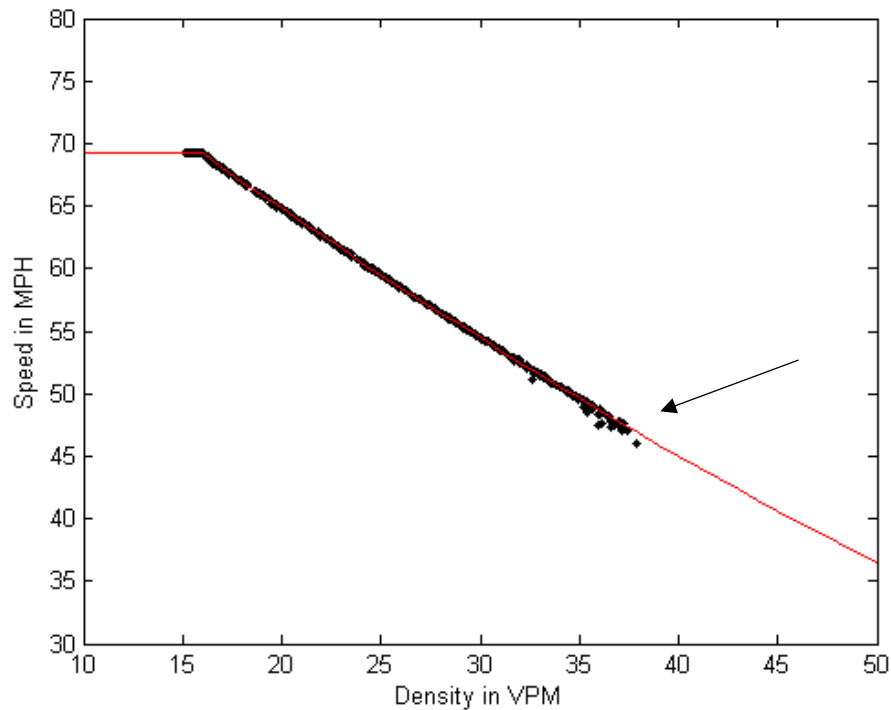


Figure 10. Speed-density results from testing car following model parameters - example of a bad fit.

As can be seen in the figures, the well-fitting results follow neatly along the entire range of the fundamental diagram between 15 and 42 vpm. In the bad fit example, only a subset of the range was acceptable during stream perturbation – densities above roughly 37 vpm (noted by the arrow) were too closely packed to allow perturbations to subside given the test car following parameters, and some dispersion at densities near 35 vpm can also be seen. Responses were too sharp, leading to crashes quickly during each simulation.

### 3.3 Data for Calibrating and Validating Shockwave Distribution

The data which was used to calibrate this methodology was drawn from the work done by Stanitsas. Shockwaves were collected from video data taken along I-35W and I-394 during the summer of 2011. Five days were analyzed: June 29, August 23, August 25, and August 30 and 31. Video was recorded across the morning peak period of each date, from 6 AM

to 9 AM. All video was then analyzed manually to identify shockwaves which were caused by vehicles traversing the lane boundary between the HOT and adjacent GP lanes. The shockwaves were counted based on which vehicles visibly slowed – those vehicles which had to apply brakes.

In the Stanitsas paper from 2014, the shockwaves were all used for calibrating and validating the model which was developed, regardless of the density condition from which they originated. A wide density region was considered by that methodology (15 to 25 VPM), and speeds on the adjacent lane were assumed to be near 35 MPH. By comparing the shockwaves which were collected against 5-minute traffic data, both the density and speed assumptions were found to be suspect.

Across the 5 days which were usable, a total of 302 shockwaves were collected. Data from a nearby loop detector station was compared against the recorded time of each shockwave, and each shockwave was assigned a HOT lane density value and an adjacent GP lane speed value. The shockwaves were then broken into groups based on what density they fell into: 15 to 18 vpm, 18 to 21 vpm, and so forth up through 30 to 33 vpm. No density conditions higher than the 30 to 33 vpm range were recorded during the observation period. These results are summarized in Table 3 below.

*Table 3. Shockwave samples and their corresponding adjacent lane conditions.*

<b>Density (VPM)</b>	<b>Number of Shockwave Samples</b>	<b>Min Speed (MPH)</b>	<b>15th Percentile Speed (MPH)</b>	<b>Mean Speed (MPH)</b>	<b>85th Percentile Speed (MPH)</b>	<b>Max Speed (MPH)</b>
15 to 18	48	15.7	16.7	19.3	24.1	34.1
18 to 21	86	16.1	16.8	21.0	24.7	33.1
21 to 24	52	17.4	17.8	21.6	23.9	34.9
24 to 27	75	15.8	16.5	21.1	24.3	30.4
27 to 30	30	16.0	16.5	20.8	24.7	28.1
30 to 33	11	16.7	16.4	19.4	23.2	28.5

Based on these groupings, each segment from 15 to 27 vpm includes a non-trivial number of samples, with only the 27 to 33 vpm groups being too small to provide an adequate comparison set for calibration and validation.

As for the speed of the adjacent lane, the conditions corresponding to shockwaves in each group were also analyzed. In each density group, the speeds on the adjacent general purpose lane were remarkably similar, as can be seen in Table 3. Regardless of the HOT condition, the adjacent speeds were between 15 and 35 MPH, with the 15th and 85th percentiles at roughly 16 and 24, respectively. Mean speeds were between 19 and 21 MPH. Thus, instead of assuming an adjacent lane speed of roughly 35 MPH, calibration within this methodology took place using speeds randomly distributed between 15 and 25 MPH, roughly capturing the common behavior of the lane. At the same time that shockwave data was collected, platoon sizes and leader/follower headway samples were taken from video data, and serve as a main input to the entire methodology.

### 3.4 Final Calibration and Validation

The data described in Table 3 were broken into two halves randomly with one set used for calibration and the other set used for validation. Final efforts to calibrate the model focused around the largest set, the shockwaves under density conditions 18 to 21 vehicles per mile. Using the Monte Carlo sampling technique and shockwave generation methodology described above, sample sets of 100 shockwave lengths were generated for varying sets of car following model and behavioral parameters. Many iterations were performed with wide ranging parameter options guided by engineering judgement of the effects of each parameter.

As calibrations were attempted, well-fitting sets of parameters were tested under other density conditions described in Table 3. It became apparent that the model was unable to achieve good fits across all densities. Two changes to the underlying car following model were introduced to allow better fits between simulation and the real data.

The first change was related to the sensitivity coefficient of the car following model. It was observed that goodness-of-fit measures were not consistent across varying density ranges when using a static set of calibration parameters – i.e. traffic behavior changes across densities between 15 and 42 vpm. Thus, a method for making the car following model dynamic based on density was introduced. Instead of a fixed sensitivity coefficient, a scaling alpha was adopted which follows the function:

$$\alpha_k = \alpha + \alpha * \frac{k-15vpm}{25vpm} \quad \text{Eq. 5}$$

where  $\alpha_k$  is the alpha value used at density  $k$ , which ranges linearly between some base value at 15 vpm to just over twice the base value at 42 vpm. This change is reasonable given that at higher densities drivers must contend with greater numbers of other drivers and respond to more stimuli than at lower densities. Thus, drivers in dense traffic are more aggressive in responding to changes in the position and speed of the vehicle in front of them.

The second change introduced also involves driver awareness and a deficiency with single-leader car following models. In actual traffic, human drivers are often capable of observing activity in front of their immediate leader vehicle. As a shockwave approaches, some drivers preemptively brake even if their leader has not yet responded to the shockwave. To mirror this behavior in the model, a ‘look ahead’ system was introduced.

A vehicle which is allowed to look ahead makes two assessments using the car following model. The typical leader-follower pair is used to determine an acceleration to implement, just as in a normal non-look ahead vehicle. However, the look ahead vehicle then performs the same calculations but replaces the leader vehicle's position and speed with measurements from the leader's leader. The car in between (i.e., the typical "leader") is not considered by the car following model. Of the two accelerations thus calculated, the more conservative is taken. This means that a vehicle is able to begin decelerating shortly after the leader's leader responds to the shockwave, gaining some valuable time to allow the shockwaves to successfully propagate.

For example, to help illustrate this, imagine a set of three vehicles closely following one another: A, B, and C. As vehicle A begins to decelerate due to a shockwave, vehicles B and C have not yet responded. In a simulation without look ahead, vehicle B would begin decelerating a short time later (once its reaction time had been reached), and vehicle C would begin decelerating a short time after that. Thus vehicle C would respond about two reaction times after vehicle A. In the look ahead scenario, both vehicle B and C would respond at approximately the same time since any change in the speed of vehicle A would trigger a response in vehicle C. Note that this response would not occur if the vehicles were widely spaced such that the 250 foot or 4 second limits imposed on the car following model were violated.

The look ahead parameter was also introduced as a variable parameter based on the density of the stream, using the same format as the sensitivity coefficient. The look ahead parameter was set given the following function:

$$LA_k = LA + 0.40 * \frac{k-15vpm}{25vpm} \quad \text{Eq. 6}$$

where  $LA_k$  is the look ahead rate at density  $k$ . The base value of LA was set to 0.05, or roughly 1 in 20 vehicles would respond using the look ahead at 15 vpm. This increases to just under 50% of vehicles at critical density.

With the two alternations indicated above, the remaining behavioral parameters taken from the literature by Stanitsas were maintained, and the new parameter of Minimum Deceleration Response was set to the value given in Table 1. The ultimate car following model parameters were set as  $\alpha = 140$  (recall that this is the base value at 15 vpm),  $L = 2.5$ , and  $M = 1$ . Thus, the car following model response is proportional to the speed of the following vehicle raised to the power of 2.5, and inversely proportional to distance between the following vehicle and its leader.

Using those values, a comparison was made using a Kolmogorov-Smirnov Two-Sample test, and cumulative distributions for both calibration/validation and simulated data were made. Figure 11 below shows the calibration results for 18 to 21 vpm, and Figure 12 shows the validation results for the same density range. Across the other density ranges, calibration/validation results were reasonable, and are detailed in Table 4.

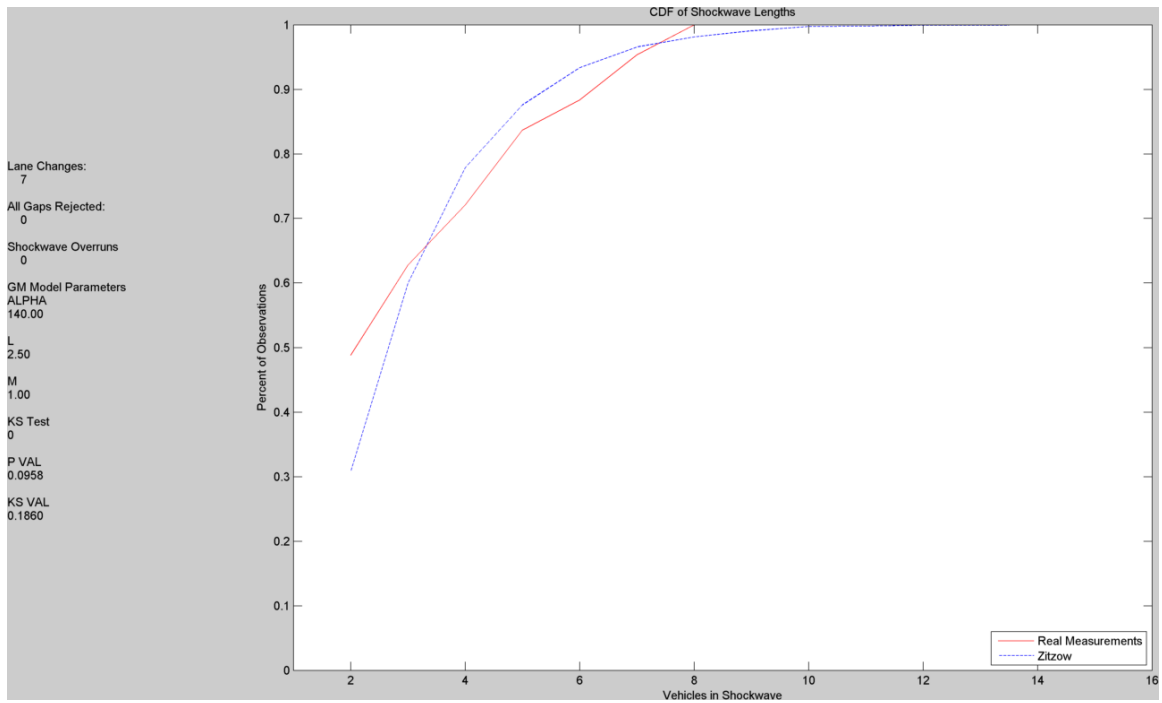


Figure 11. Cumulative distribution results for calibration using shockwaves in the 18 to 21 vpm density range.

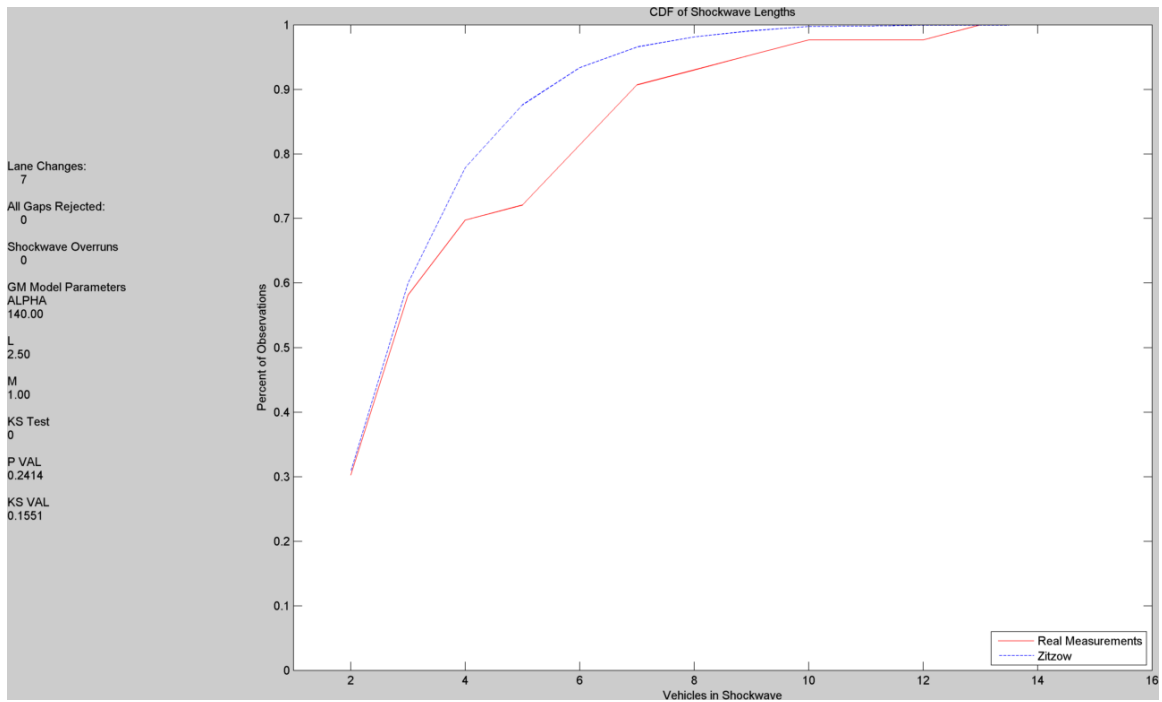


Figure 12. Cumulative distribution results for validation using shockwaves in the 18 to 21 vpm density range.



Table 4. Calibration and validation results.

Density Range	# of Total Samples		Calibration Success	KS-Statistic	Validation Success	KS-Statistic
15 to 18 VPM	48		No	0.3333	Yes	0.2427
18 to 21 VPM	86		Yes	0.1860	Yes	0.1551
21 to 24 VPM	52		Yes	0.2381	Yes	0.2381
24 to 27 VPM	75		No	0.2818	No	0.4838
27 to 30 VPM	30		Yes	0.1255	No	0.4138
30 to 33 VPM	11		Yes	0.2510	Yes	0.3578

As can be seen above, the calibration and validation results show good fit for the 18 to 21 vpm range. Additionally, calibration and validation were successful for 21 to 24 vpm and, although based on extremely limited data, the 30 to 33 vpm range. Two ranges (15 to 18 and 27 to 30 vpm) each failed only one of the two checks, indicating that the parameters are likely close to a fit, but are not perfectly calibrated. The only density region which failed entirely to correspond with real data was the 24 to 27 vpm range.

## Chapter 4 - Characteristic Distributions

The shockwave distribution generation methodology laid out in the previous chapters provides a means for examining possible behavior of any given location within a HOT lane facility. Reconstructing a shockwaves for the entire corridor holistically, however, requires some additional structures which will be described in this chapter. In particular, a HOT lane corridor experiences a wide variety of conditions across different locations at any given time, and also collectively throughout a longer period of time. Simulation and historical analysis can be combined to form a complete picture of the entire corridor.

This chapter covers the simulation side of this union, including the development of several iterative layers to develop useful shockwave distributions for a variety of conditions. These particular distributions, termed characteristic distributions for this research, describe shockwave behavior on the HOT for conditions ranging from free-flowing traffic to heavy congestion. Each individual shockwave distribution is “characteristic” of a given roadway state.

This chapter focuses on building up a single set of characteristic distributions. As was noted in the previous chapter regarding calibration, individual locations within a corridor may vary based on the fundamental relationship between speed, density, and flow which is observed. Since the characteristic distributions which are created in this chapter are reliant upon the fundamental diagram relationship as an input parameter, new sets of characteristic distributions must be generated for any locations which differ from one another. In other words, if a corridor has two major sections which have differing fundamental relationships, two sets of characteristic distributions would be necessary. This

will be revisited when building a corridor-wide assessment of shockwave activity. For now, only a single characteristic distribution set is considered.

#### 4.1 Building the Characteristic Distributions

Similar to the real data described in the previous chapter, shockwave behavior changes across varying densities, but also changes depending on the speed of the adjacent lane. Broadly speaking, increases in HOT lane density lead to increasingly long shockwaves since vehicles are more closely spaced and thus are more likely to respond to one another, and decreases in GP lane speed also lead to increased shockwave length since the new vehicle entering the HOT must negotiate a larger speed differential and the resulting shockwave starts with greater ‘power.’

The characteristic distributions which will be used in following chapters to aggregate corridor behavior are broken into small regions so that the shockwave distribution within each region is stable. Overly small regions may not add new information, for example adjacent cells with near-identical distributions, but regions which are too large could miss important behavioral changes in the shockwave distribution pattern of a corridor. Thus, the 3-vpm wide density divisions were adopted throughout this methodology, prior to any calibration or examination of real data. The real-world impact of a 3-vpm change in density is one additional vehicle within every 1800 foot distance, which is negligible relative to the randomness introduced in stream generation.

In terms of speed, 5 mph pieces were selected with a similar assumption process to density. Vehicles within a lane do not all travel at exactly the same speed - the prevailing speed of the lane is somewhere within a distribution. It is not unreasonable to assume that

a large set of drivers within the same lane could vary by one or two miles per hour above or below such a prevailing speed without altering their behavior significantly.

Both of these assumed increments will be discussed again shortly in relation to the actual characteristic distribution generated in the following section.

#### 4.2 Calibrated Characteristic Distributions

Using the calibration factors found in the previous chapter, and including the adjustments to the look ahead parameter and sensitivity coefficient of the GM car following model based on density, a set of characteristic distributions were created by iterating across all speed-density conditions between 15 and 42 vpm and 10 and 45 mph using 3 vpm and 5 mph increments. The resulting characteristic distributions are shown in Figure 13.

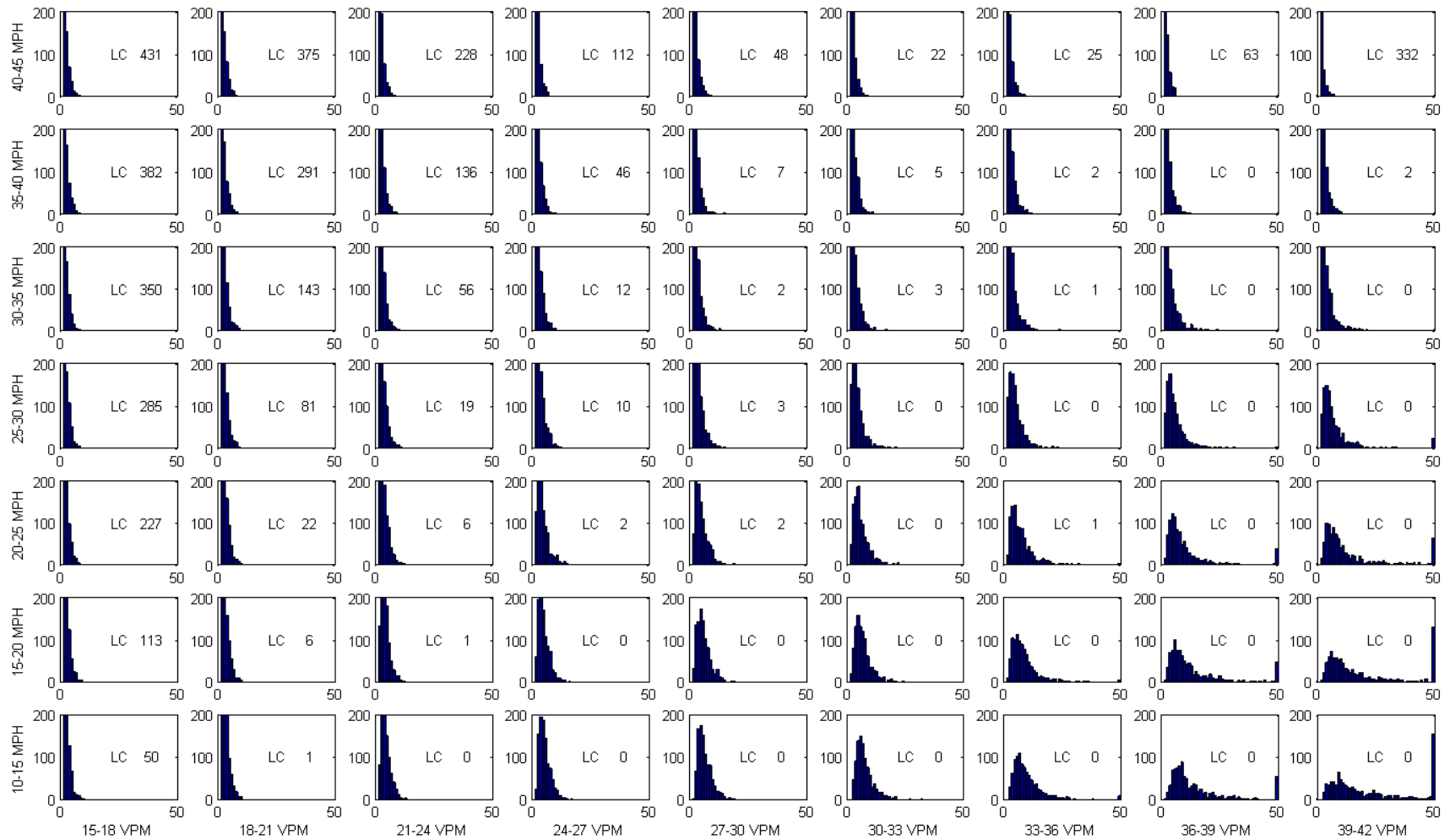


Figure 13. Characteristic distributions based on the calibrated car following parameters.

As can be seen in the figure, shockwave distributions change dramatically across the ranges of interest. For each column the density range is indicated at the bottom, and for each row the speed range is indicated at the left. Each histogram breaks the simulated shockwaves up by individual length, and shows the range from zero to shockwaves of 50 vehicles long or more. Any shockwaves longer than 50 vehicles are aggregated into the 50 vehicle count. Every histogram was generated using 1000 simulated shockwave lengths. The LC number indicated in each cell is the number of attempted shockwaves which resulted in no response within the HOT lane – i.e., the entering vehicle moved into the lane and accelerated to speed without disturbing the vehicle behind it whatsoever.

Several important things can be observed within the characteristic distribution figure. It is clear that behavior changes dramatically from low densities to high densities. This follows what would be expected. At high density on the HOT lane, entering vehicles are likely to cause significant shockwave activity since the lane is close to capacity and any moderate disturbance could cause congestion to set in. The simulated results for the lower right-most cell indicate that roughly 150 of the recorded shockwaves were 50 vehicles long or more and just over one-third were 25 vehicles or longer. Moving up the far right column, shockwave lengths become significantly smaller in the top three rows. Under those conditions, speeds on the adjacent lane are between 30 and 45 mph. However, by examining the fundamental diagram relationship between speed and density on the HOT lane which was calibrated in Chapter 3, the speed on the HOT falls to between 40 and 45 mph. Thus the speed differential in the far right column changes from near zero at the top to about 30 mph at the bottom. Also note that in the upper right corner, a third of vehicles

entering the HOT make no disturbance to the stream because the two lanes have harmonized speeds.

These findings raise some question regarding the use of 3 vpm and 5 mph segments. Clearly, the adjacent cells in the characteristic distribution function show notable changes. Using the Kolmogorov-Smirnov Two-Sample test between adjacent cells across the data shown in Figure 13, few of the distributions are close enough to one another to be considered comparable. However, in light of the inherent error within the historical data which will be integrated with this methodology in the following chapters, these concerns will be set aside for this research.

## Chapter 5 - Assessing Historical Data

While the characteristic distributions which have been developed capture the behavior of vehicles under certain combinations of HOT lane density and adjacent general purpose lane speed, these data are not useful for understanding the overall behavior of a corridor without some measure of what conditions actually take place on the roadway. This chapter lays out the methodology which was developed to account for historical traffic data and combine the characteristic distributions into a single unified measurement for a given location.

The Monte Carlo framework and the data that underpin it were all collected and aggregated based on a 5-minute time increment. This particular increment was selected to reduce the high variability of traffic data from a lower time step (such as the native 30-second data which is produced by the Twin Cities detector system), while maintaining sufficient resolution to capture important variation in density and speed which occur over time. For consistency, 5-minute data is again used within this assessment methodology. Finally, this chapter ostensibly focuses on historical data for an existing roadway, and will consistently refer to the data which is examined as historical, but the same tools could just as easily be used for a hypothetical corridor using simulated traffic data.

The goal of this assessment is to establish the relative frequency of every pair of conditions which occur within a particular segment of a corridor. In keeping with the development of the characteristic distributions from the previous chapter, density is broken into 3-vpm segments and speed is broken into 5-mph segments. However, for a complete picture of the behavior of the location, all possible speed/density combinations will be considered. Thus, instead of limiting density (on the HOT) to between 15 and 42 vpm and



speed (on the GP) to between 10 and 45 mph, densities between 0 and 240 vpm will be tabulated and speeds between 0 and 100 mph. Note that the upper boundaries of these two ranges are much higher than are likely necessary to capture all the reasonable data for the corridor.

Recalling the findings of the characteristic distribution regarding the segmentation of density and speed from the previous chapter, the variability of traffic measurements is important to discuss. As noted, the variability of traffic data collected by single-loop detector stations is significant. Imbalances in vehicle lengths throw speed estimations off, consequently causing error in density calculations. Thus, the assumed logic behind selecting those segmentations – that neither a couple extra vehicles per mile nor a handful of miles per hour make a significant difference in driver behavior – remain in effect.

With this framework in mind, successive days of historical data can be examined and each 5-minute data point can be added to the appropriate ‘bin’ within the speed/density matrix, building up a 2-dimensional histogram of past conditions. This histogram can then be transformed into relative percentages by dividing the total in each bin by the total across the entire array. These percentages are the relative frequency of each condition appearing on the roadway. However, the relative percentages across this array may or may not be representative of the behavior of the roadway over time. In order to determine if sufficient sample days have been added, a mean squared difference index is implemented which, when sufficiently minimized, indicates that the frequency chart has converged.

For every bin, two values are compared: the frequency of that bin for all days 1 to N, and the frequency for that bin for all days 1 to N-1. It is important that the counts in each bin are first transformed into a relative frequency since, as each day is added,

individual bin counts continue to grow and do not find convergence. By instead looking at the relative frequency, convergence is possible. Figure 14 below illustrates the process.

User Input

<i>Corridor Parameters</i>
<ul style="list-style-type: none"> <li>• Paired HOT and Adjacent General Purpose Lane Detector IDs</li> <li>• Single-Loop Detector Field Lengths</li> </ul>

<i>Date Range and Days-of-Week (optional)</i>
<ul style="list-style-type: none"> <li>• Specific Date List</li> <li>• Specific Days-of-Week inclusion</li> </ul>

Assess Real Data

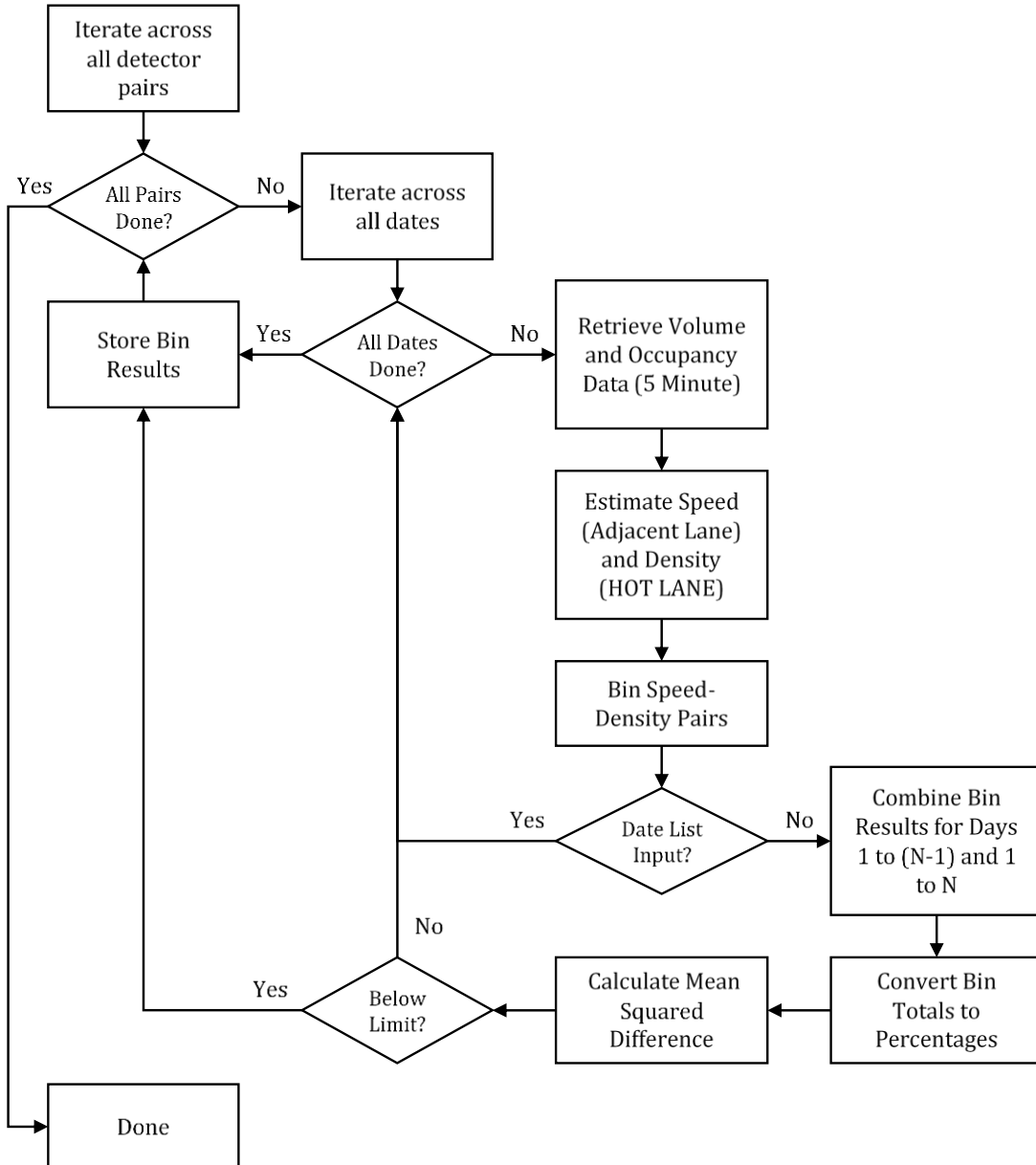


Figure 14. Flow diagram for assessing historical data.

This method was used for the Cliff Road location on I-35W, taking data from September 1, 2015 to November 30, 2015 to build the relative frequency mapping. Based on those data, Figure 15 shows the relative frequency as a contour map across density on the HOT and speed on the GP. Two main peaks are present within the data, one at very low density (between 2 and 3 vpm) and high speed, and a second weaker peak at roughly 12 vpm and free flowing conditions. A significantly weaker peak can just be seen inside the characteristic distribution range (outlined in dashed red). The characteristic distribution range will be focused on more closely in a moment.

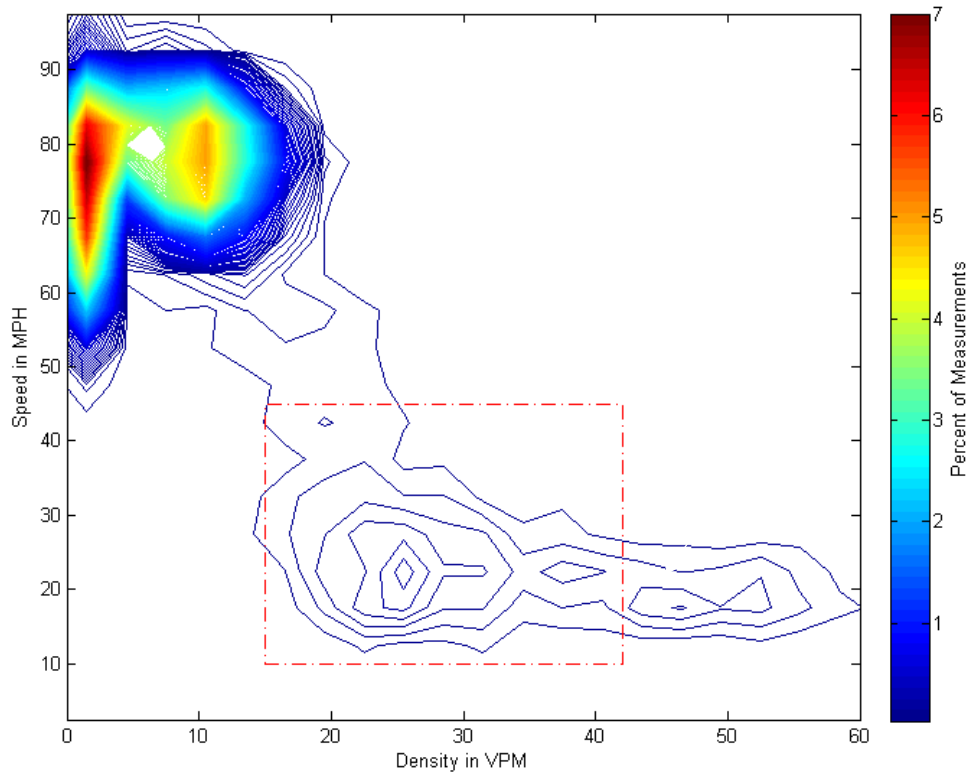


Figure 15. Contour plot of historical data.

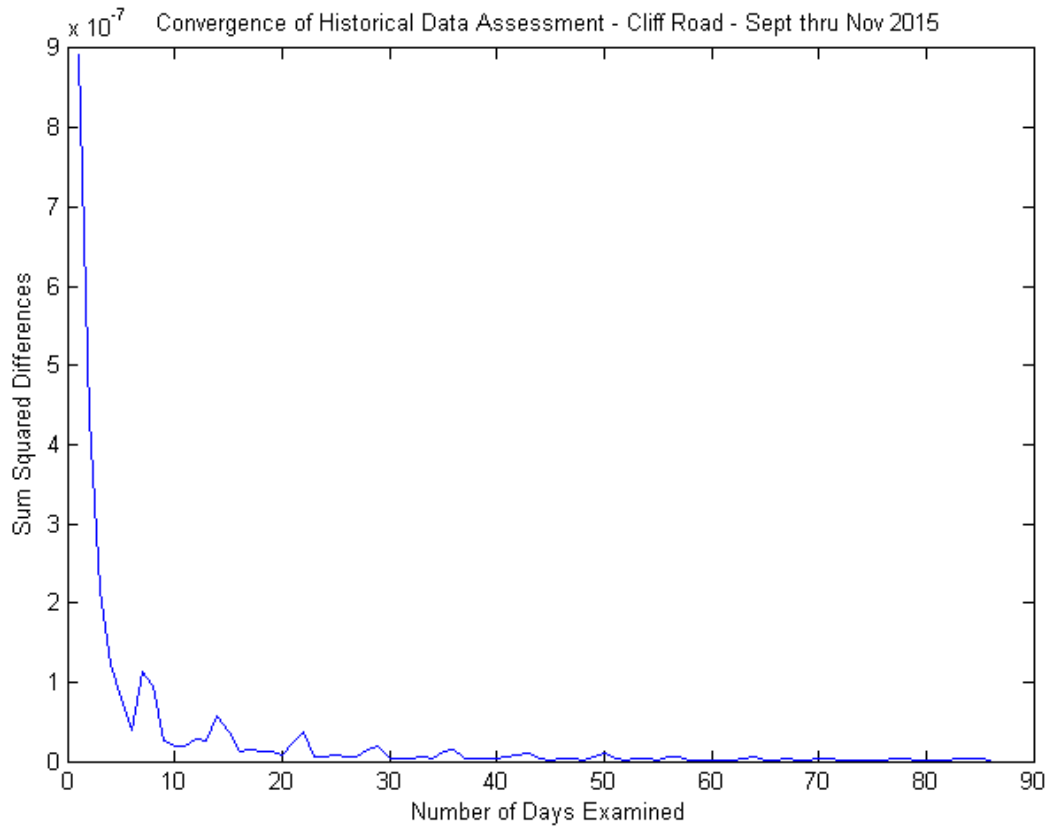


Figure 16. Convergence of historical data.

Figure 16 above shows the mean squared difference as successive days of data were added to the frequency calculation. After only a few days the mean squared error dropped significantly, continuing to improve until a rough convergence between 50 and 60 days of data had been incorporated. The small ‘hiccups’ in the mean squared error indicated in the figure are caused by each weekend within the data, which includes a markedly different frequency pattern from weekdays. To correct this, Figure 17 and Figure 18 below only include weekdays.

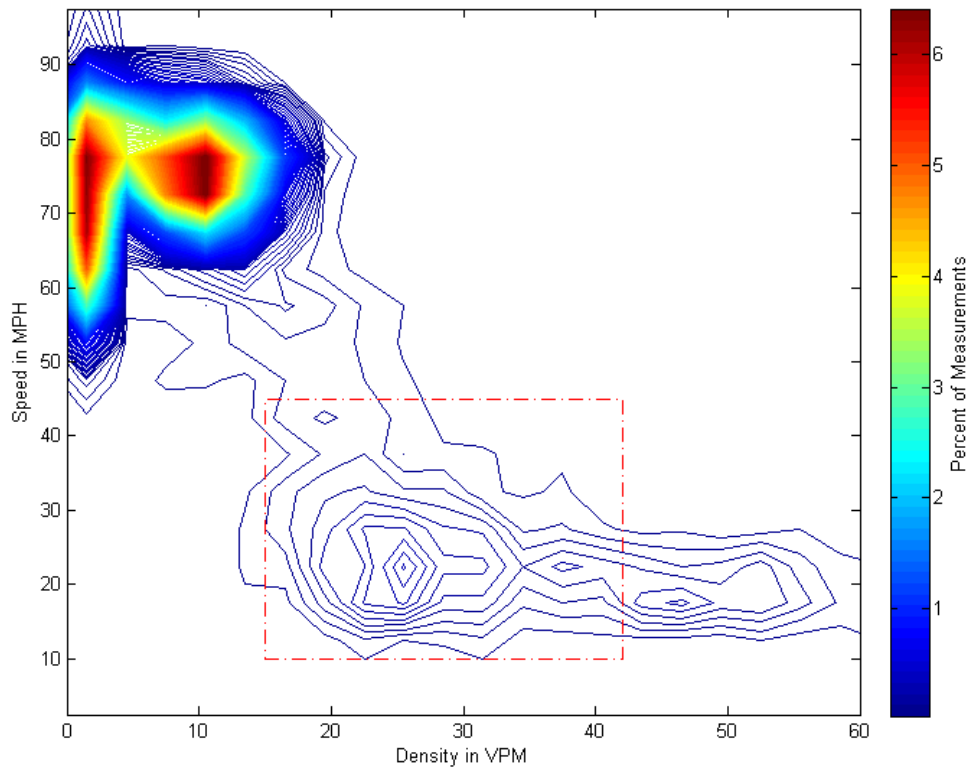


Figure 17. Heat map of historical data excluding weekends.

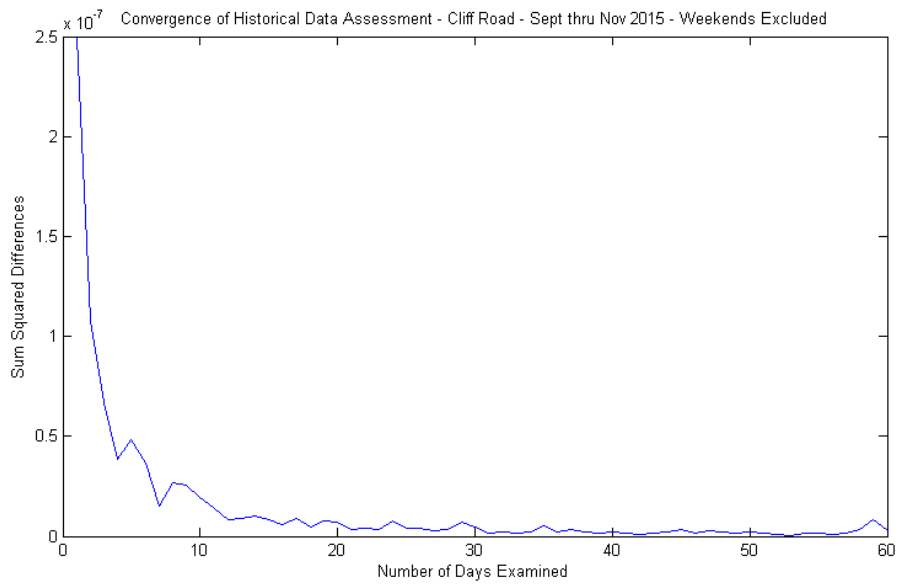


Figure 18. Convergence of historical data excluding weekends.

Removing the weekend dates clarifies the peaks found within the contour figure. This is sensible since nearly no time during weekend days would experience significant activity on the general purpose lanes, much less the HOT. Figure 18 also shows an improvement in convergence, which is reached with no further major hiccups after roughly 35 days, rather than 50 or 60 days when weekends are included. The overall sum of squared differences also notably improves.

The figures shown above are based on the full range of data. However, prior to moving into the next chapter, one last adjustment must be made. Only the data corresponding to the characteristic distributions will be directly manipulated to produce cumulative results. Thus, those data are excised from the full data set. Figure 19 below shows the resulting contour figure which results from using only that subset of data to calculate relative prevalence.

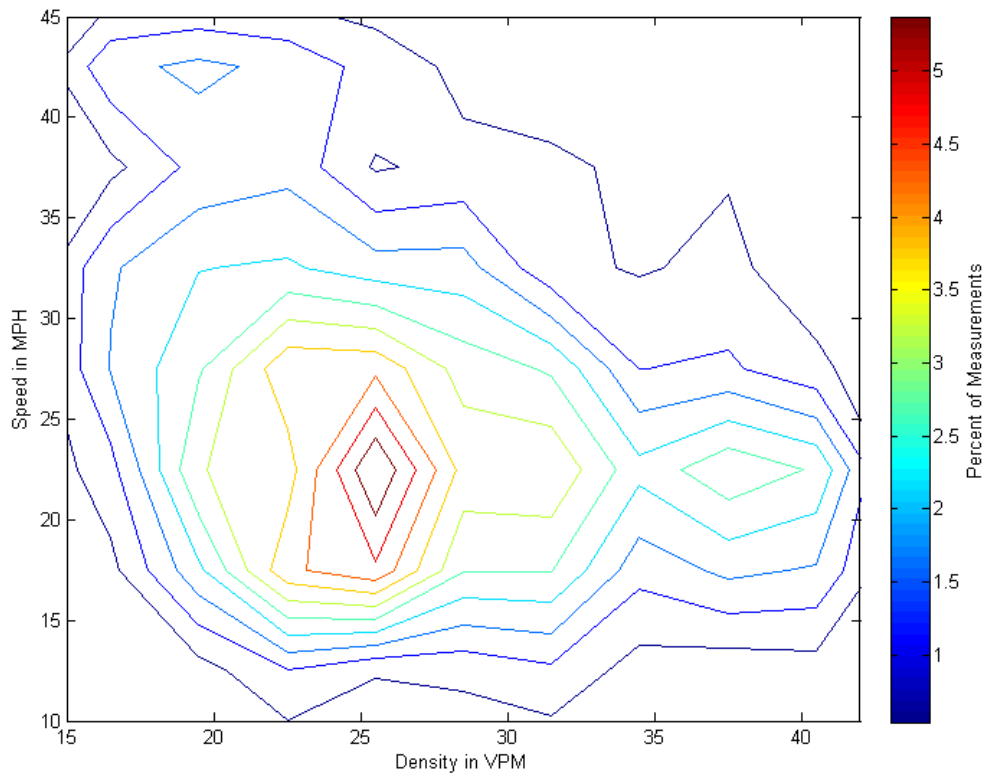


Figure 19. Heat map of historical data within the characteristic distribution speed-density range.

A strong peak is seen at the 24-27 vpm and 20 to 25 mph condition, with a minor peak at 36 to 39 vpm and 20 to 25 mph. The percentages noted in the figure will come into direct use in the next chapter.

### 5.1 Density Increase Scenarios

One major question which this methodology seeks to aid in answering relates to future conditions on an existing HOT facility. As traffic grows year to year within a corridor, higher extreme density conditions occur, and moderate to high density conditions are broadly expected to occur more frequently as well. Managers of HOT lanes may be forced to increase the load on the managed facilities to help offset mitigate congestion in the general purpose lanes.



Using the same historical data as above, three new increased density data sets were constructed to explore such future conditions. These test data sets were constructed from the actual detector data which was described above, but with modifications to the densities on the HOT lane. Since these tests are meant to examine heavier loading on the HOT lane (likely due to managers modifying the tolling rate on the lane or general increased demand for the lane), only the density value of each 5-minute data point was manipulated leaving the speed on the general purpose lane unaltered. The three test scenarios incorporate a 50%, 75%, and 100% increase in density on the HOT.

Thus, for example, a 5-minute data point which measured a HOT lane density of 19.3 vehicles per mile and an adjacent GP lane speed of 37.9 miles per hour would be modified into a data point with a HOT lane density of 28.95 vpm under the 50% increase scenario, 33.78 vpm under the 75% increase scenario, and 38.6 vpm under the 100% increase scenario. In each of those increased scenarios, the speed on the GP remains at 37.9 miles per hour. Thus, the data which was used to develop Figure 17 is modified to appear as shown in Figure 20 below.

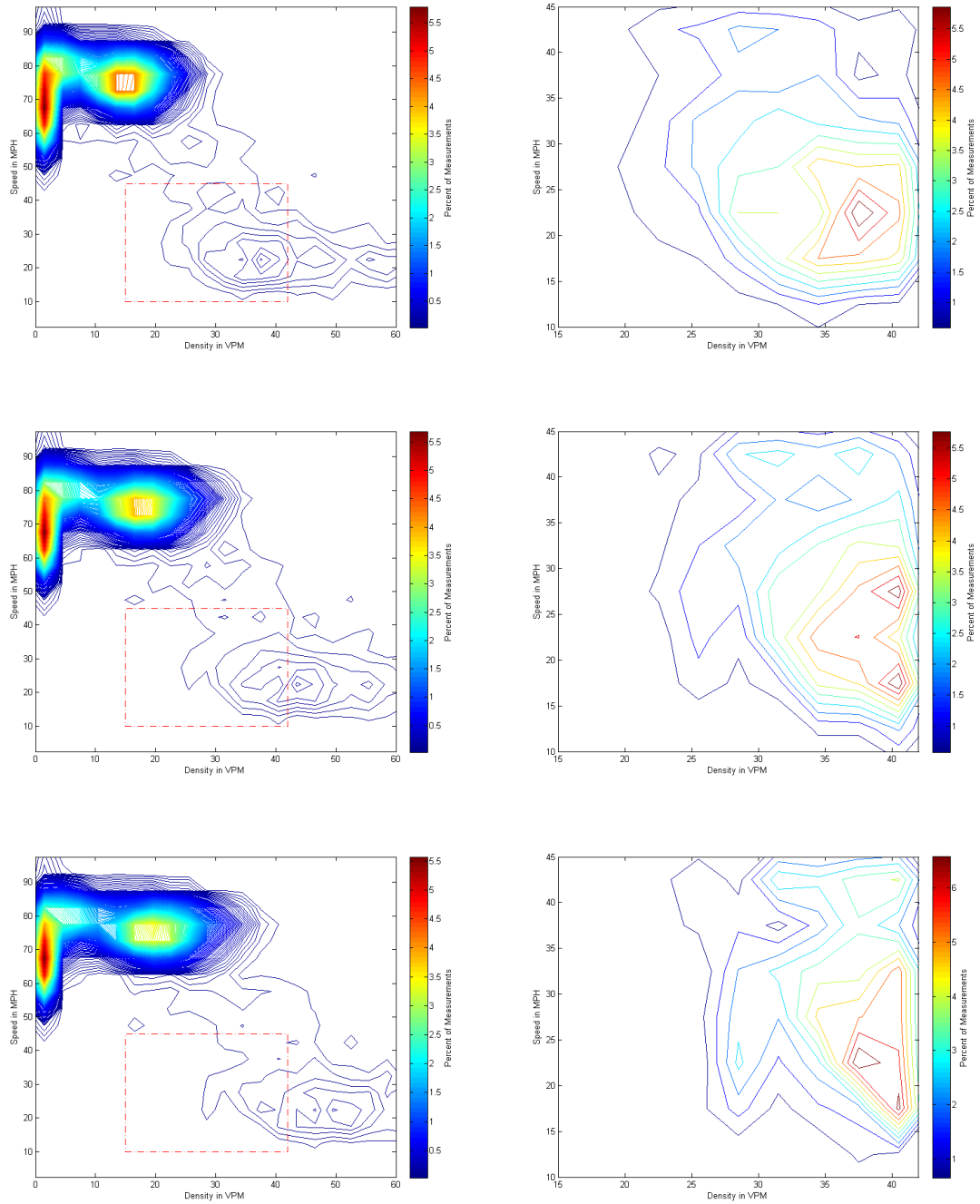


Figure 20. Increased density scenarios: 50% increase (top), 75% increase (middle), and 100% increase (bottom).

The figure shows a modest shift in the high-speed peak within the complete data set in each subfigure on the left side. The circular peak with a strong center gradually moves rightward and flattens, as expected. Similarly in the right side subfigures, the peak

within the characteristic distribution range moves notably rightward. However, unlike the overall data, the sharpness of the peak increases in the 75% and 100% increase scenarios. Again, the data contained within the subfigures on the right hand side will be instrumental in the following chapter.

## 5.2. Peak Periods Only Consideration

A last possible dataset of interest includes only the AM and PM peak periods of a corridor. Since those periods are the most likely to have major congestion, and use of the HOT lane for commuting purposes, especially for those going home from work in the afternoon, is greatest. By restricting to the peak periods, a more concise idea of the historical behavior of the HOT and adjacent general purpose lane can be formulated. For this consideration, AM peak is 6 AM to 10 AM and PM peak is 3 PM to 7 PM.

For the Cliff Road segment used in previous sections, the restricted data form a heat map of speed-density conditions as shown in Figure 21.

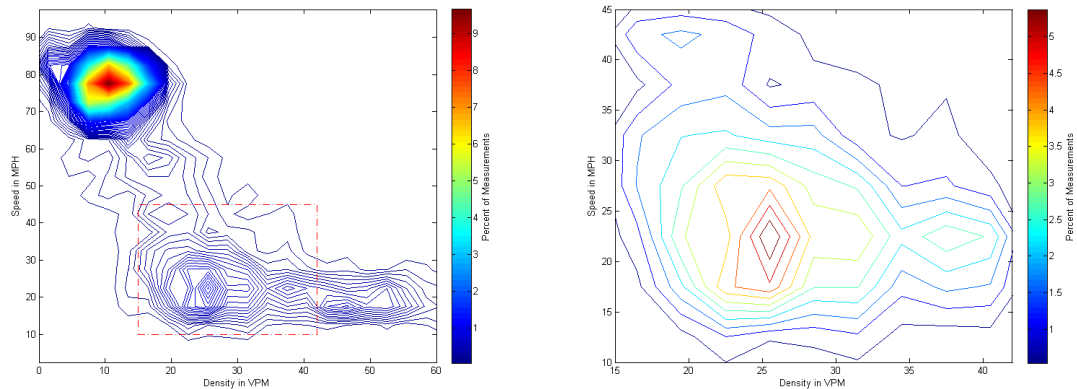


Figure 21. Heat map of peak period only data for Cliff Road considering full ranges of speed and density (left) and only the characteristic distribution region (right).

The results bear a strong similarity to the figure including data from all day. One major difference in the subfigure at the left which includes the full range of speed and density possibilities is the missing vertical streak at extremely low density. During peak

periods, there is generally some modest density even on lower traffic days. Thus the strong peak at high speed and falling around 10 vpm in the HOT. The subfigure at the right capturing only the portion of data which falls within the characteristic distributions is virtually unchanged. This is reasonable given that the majority of instances where the mainline breaks down and a higher density of traffic is observed on the HOT is during peak periods. Some off-peak occurrences may happen, possibly due to special events, weather, or traffic incidents, but those are relatively rare. This examination of peak period versus full day data will be revisited in the following chapter when full corridor-wide results are generated.

## Chapter 6 - Corridor-Level Assessment Tool

The ultimate goal of the methodology in this research is to examine the entirety of a corridor within one framework and produce a comprehensive assessment of the shockwave behavior of a complete HOT lane facility. This is achieved by combining the methodologies presented in the preceding chapters: the characteristic shockwave distributions produced by the Monte Carlo sampling methodology for each of the speed/density conditions of interest are combined with the historical assessment distributions for each location along the corridor to generate a single mapping of shockwave activity throughout.

These corridor maps can then be assessed holistically to identify locations where shockwaves of notable length occur frequently and thus which locations may require treatment to improve safety within the corridor. Since no direct correlation between shockwaves and crashes has been developed, this tool serves to inform the designers or operators of a HOT lane facility and to aid in their engineering judgement of the safety of the corridor.

This chapter brings the methodologies already presented together into a unified whole, first by creating a comprehensive shockwave distribution based on historical data for a single location within a corridor, then by extending throughout the entire corridor. The overall method is laid out and a complete example is given, including increased density scenarios as described in Chapter 5, for a part of I-35W in Minneapolis, Minnesota.

As was noted at the beginning of Chapter 4, characteristic distributions are dependent upon the fundamental relationship of each location in a corridor. Where before assuming a single relationship was sufficient to explain the development of arbitrary

characteristic distributions, this issue must now be revisited. An examination of the fundamental relationship for each station throughout the entire I-35W corridor described in Chapter 5 was performed. Overall, the corridor appears to have two broad sections which behave slightly differently, separated by Highway 62. South of Highway 62, the fundamental diagram is very close to the fitted relationship from Chapter 3. North of Highway 62, speeds drop more quickly as density increases, as seen in Figure 22 below.

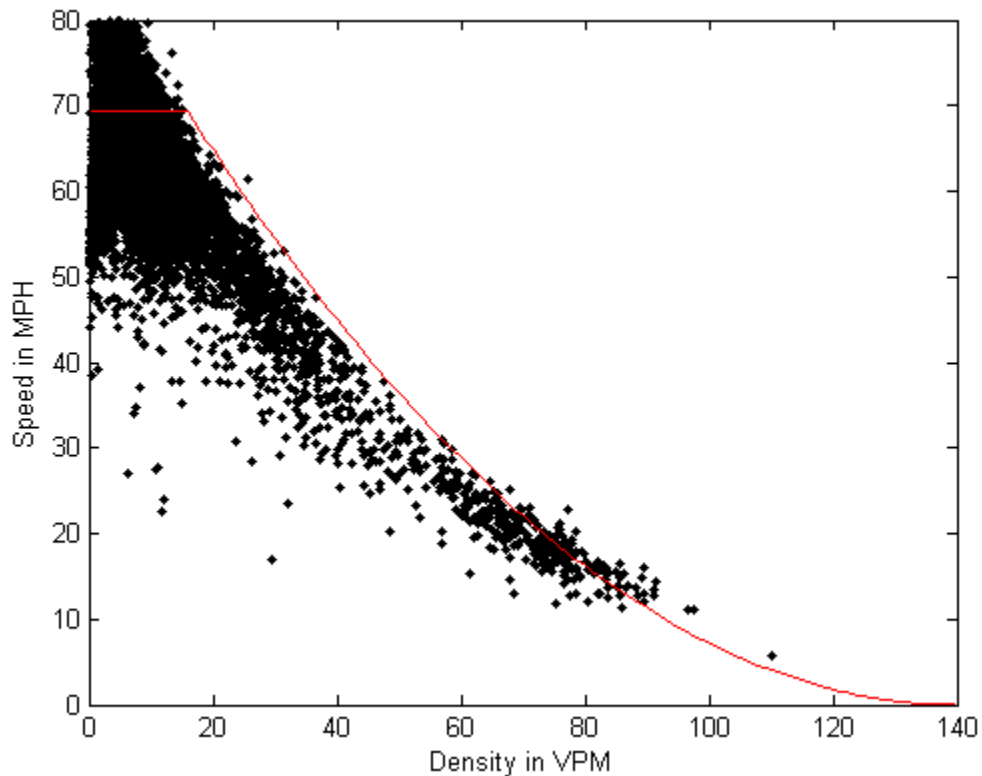


Figure 22. Comparison of real data and Cliff Road fitted curve for location north of Highway 62.

For any given density, the curve which was fit using Cliff Road is roughly 5 mph higher than the approximate middle of the point cloud. Due to time constraints, this difference was not incorporated into the final results described below. Essentially, the 5 mph offset in Figure 22 would shift data down the characteristic distributions one row. Based on the characteristic distributions which were generated using the fit from the Cliff

Road data set, a 5 mph shift downward would slightly increase longer shockwaves for the region north of Highway 62.

### 6.1 Comprehensive Shockwave Distributions

At a single location, historical data and characteristic distributions are cross-referenced to compile what will be referred to as a comprehensive shockwave distribution. Essentially, the characteristic distributions are ‘weighted’ based on the historical data for the location and the relative frequency with which each of the characteristic distribution conditions occur on the roadways. Two calculations are made for each location: the weights are applied to the characteristic distributions to assemble the comprehensive shockwave distribution, and the percentages of all data falling in certain larger regions across speed and density are found.

The first of these calculations is essentially self-explanatory. The percentages which were generated in Chapter 5 describing the frequency of occurrence of any of the density-speed conditions in the historical data are multiplied directly against the characteristic distributions for the corresponding conditions. Thus for a speed-density pairing which represented 5% of historical measurements the histogram values for the related speed-density characteristic distribution would each be multiplied by 0.05. If 100 of the sampled shockwaves were of length 3, this would transform into 5 shockwaves of length three.

Following this multiplication, the resulting shockwave ‘counts’ for each shockwave length are combined in the comprehensive shockwave distribution for the given location. For example, the 5 shockwaves of length 3 already found, which represent the contribution of one particular speed-density condition, would be added to the 10 shockwaves of length 3 found for an adjacent speed-density condition (perhaps coming from a characteristic

distribution containing 40 shockwaves of length 3, but with a historical representation of 25% --  $40 * 0.25 = 10$ ). This same approach is repeated across all shockwave lengths for all characteristic distribution speed-density condition pairs, ultimately yielding a single combined shockwave length distribution which encapsulates both the simulated behavior of the corridor under arbitrary conditions and the historical data of the corridor which describe how the location actually performs.

For example, using the historical data for the Cliff Road station along I-35W, the following comprehensive shockwave distribution (see Figure 23) was developed. The calibrated characteristic distribution cells were each multiplied by their corresponding percentages and aggregated, resulting in the unified estimate of shockwave behavior at Cliff Road.

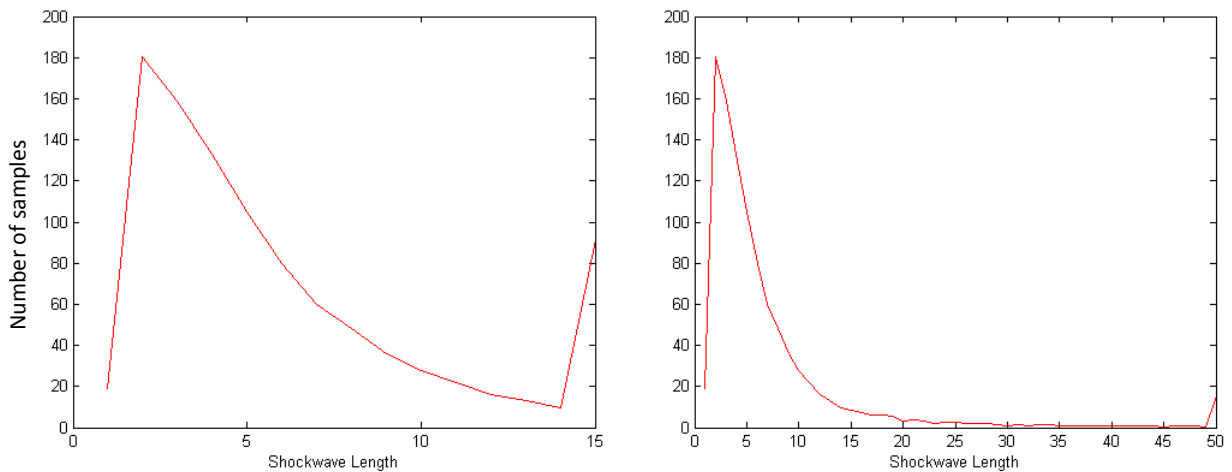


Figure 23. Comprehensive shockwave distribution for only Cliff Road.

From the figure it can be seen that the major peak in shockwave length is at two and three, but a small bump in shockwaves of length 15 or more is observed. That peak captures the relatively rare circumstances where the GP lanes are broken down and the HOT is functioning in such a way as to make the formation of longer shockwaves likely –



i.e., the HOT density increases significantly. On the right side of the figure, the shockwave lengths are extended to show this long tail out to 50, with a small bump again indicating that more shockwaves are longer than 50 vehicles.

The second calculation which is done when assembling the comprehensive shockwave distribution deals with the regions not covered by the characteristic distributions. Recalling from Chapter 2, Figure 24 shows the full ranges of speed and density broken into four major regions which must be considered separately.

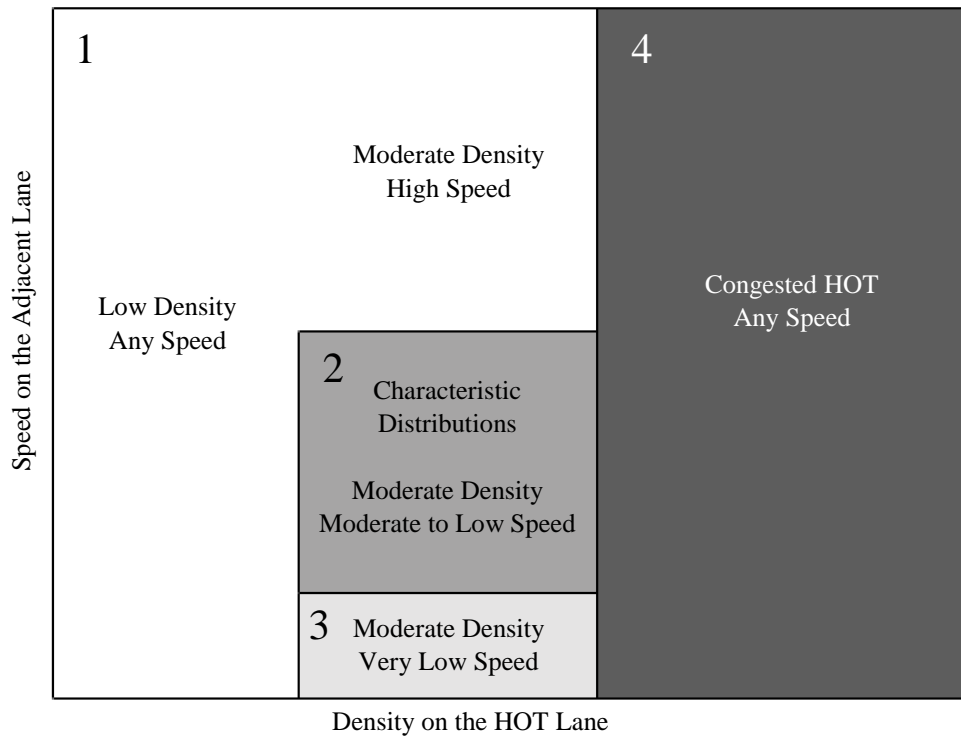


Figure 24. Important speed-density regions.

The four components illustrated above represent major regimes which can be considered separately. The white area includes both a region above the characteristic distribution, where speeds on the adjacent GP lanes are higher than 45 mph but the density on the HOT in between 15 and 42 vpm, and the region covering densities from 0 to 15 vpm

at any speed on the adjacent lane. Under those conditions, shockwaves on the HOT are either unlikely or will be short and vehicles will not involve a significant speed drop. Historical data which falls into the white area can be considered as 'safe' from the perspective of this analysis.

The next region, found in the center of the figure, is the characteristic distribution range of densities (15 to 42 vpm) and speeds (10 to 45 mph). Data falling within those ranges is already well-considered by this methodology. Underneath the characteristic distribution is a region which represents virtually stopped traffic on the general purpose lane and a notable density on the HOT. This third region is potentially extremely dangerous for drivers attempting to transition between lanes due to the severity of the speed drop. Any notable occurrence of region three within historical data may suggest a need for lane change prohibitions.

Finally, the region to the right of 42 vpm indicates that the HOT has broken down into congested behavior and the tolling function on the lane has failed. Ideally, a well-managed lane would never reach region four. Under the cases where it does, the HOT operates as another lane within the freeway system and lane changing behavior is no more significant than across the other general purpose lanes.

Finding the relative percentages of data which fall into each of the four regions can help to define the operating condition of the HOT facility. Areas within a corridor which experience a high percentage of region 4 indicates a bad tolling algorithm or a location which simply cannot cope with the given demand. High percentages of region 3 similarly could indicate a tolling system which is not functioning properly – by setting the toll too high, capacity is being wasted while the general purpose lanes are at a standstill. These

percentages will be considered again in the next section when considering corridors on a holistic basis.

## 6.2 Corridor Level Analysis

The final extension of the methodology is to repeat analyses across space to develop a corridor-wide evaluation of shockwave activity. The characteristic distributions which were created in Chapter 4 incorporate certain traffic behavior parameters and were calibrated to match with data taken from a real area. These parameters are assumed to be consistent throughout a given corridor – the drivers and roadway are similar, thus responses are similar. As a result, the same set of characteristic distributions are used in conjunction with historical data from each location (in this case, each detector station) within the corridor to create comprehensive shockwave distributions. Only the historical data and relative percentages for each density-speed condition change; the characteristic distributions underlying the calculations remain constant throughout the corridor.

Iterating across a corridor creates a three-dimensional result dataset: along the x-axis is shockwave length in vehicles, along the y-axis is distance along the corridor marked by each station, and the z-axis represents the number of shockwaves in the comprehensive shockwave distribution for each location. Again, this z-axis value is the sum of the characteristic distribution shockwave lengths weighted by the historical data percentages. Figure 25 shows a sample surface rendering of the data for I-35W.

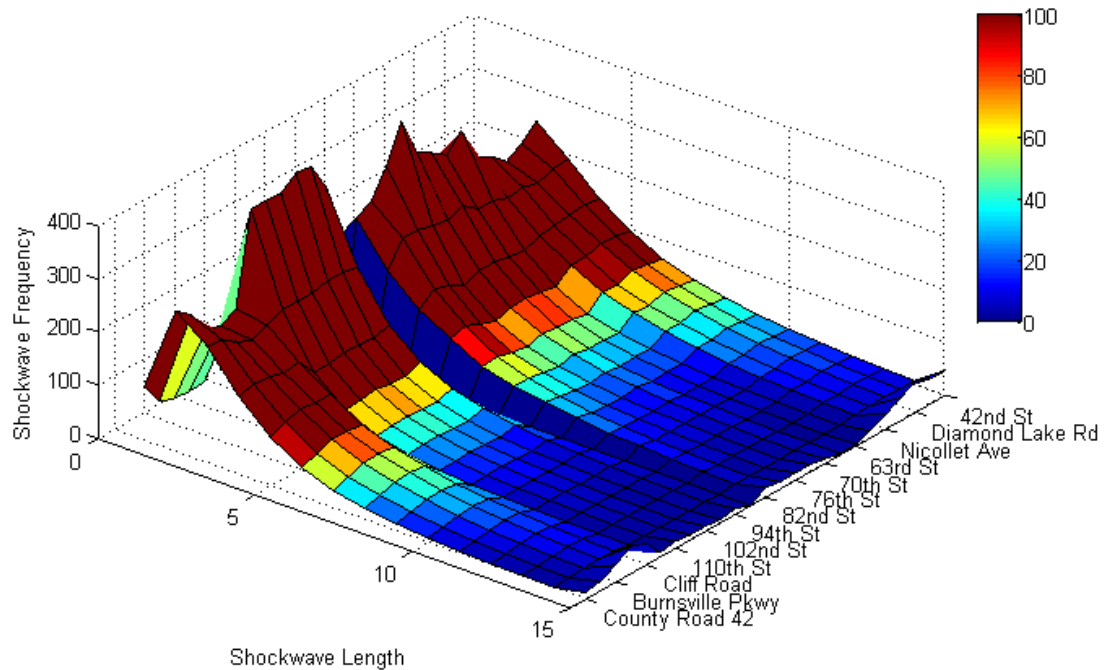


Figure 25. Surface rendering of comprehensive shockwave distribution.

As can be seen in the figure, most of the shockwaves throughout the corridor fall in the 2-5 vehicle range (indicated in dark red). However, there are two locations within the corridor where higher length shockwaves are more likely. Those can be seen as ridges extending out to near 10-vehicle long shockwaves, at the Burnsville Parkway to Cliff Road and 42nd Street to Diamond Lake Road regions. At those locations, the peak at 2-3 vehicle shockwaves is significantly lower than elsewhere in the corridor, and a higher number of long shockwaves are also expected. There is a gap in the middle of the figure at 85th Street. At that location, the detector station did not have any data which fell in the characteristic distribution range of speed and density.

It is important to note that the results in Figure 25 are only useful to describe relative shockwave prevalence. The characteristic distributions which were used to create the figure included 1000 shockwaves per speed-density condition. Those were then multiplied

by percentages according to the historical data and summed to create a total number of shockwaves per length per location. If only 100 shockwaves per speed-density condition had been used, the totals would have been exactly 1/10th of those shown. I.e., the figure would range from 0 to 40 shockwaves on the z-axis instead of 0 to 400. However, the relative heights of each of the peaks would remain the same.

Although the surface rendering does illustrate the situation, it can be difficult to interpret since parts of the region can be obscured. Instead, a heat map version can be created displaying the same information. Figure 26 shows the same data as Figure 25 , just from the top down.

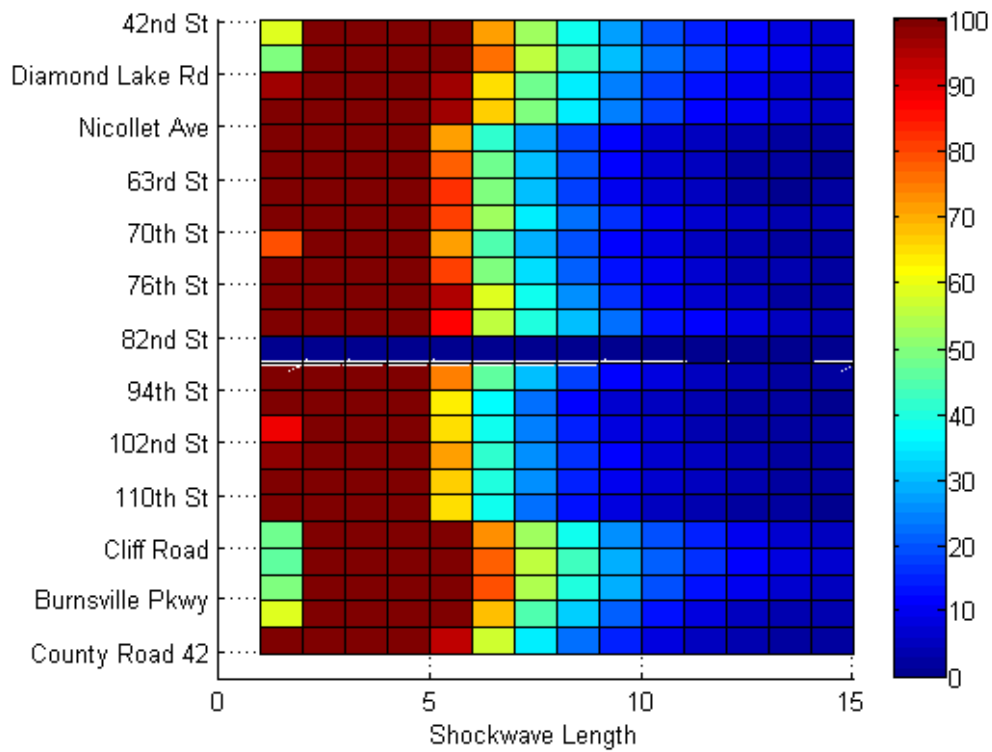


Figure 26. Comprehensive shockwave distribution using full day historical data.

In Figure 26, the dramatic difference in peaks between Cliff Road and the surrounding area is not displayed since the coloring truncates values above 100. This allows the figure to distinguish the increased prevalence of longer shockwaves at the two

aforementioned locations. Lighter blues can be seen extending throughout the 10 to 15 shockwave-length range around Cliff Road and 46th Street, with a weaker signal at the I-494 interchange near 82nd Street.

Although this methodology does not directly indicate a cutoff between safe and unsafe conditions, a framework for how those cutoffs could be determined is possible. For example, if a correlation between crashes and shockwaves of length 10 or more were established, a roadway manager could set a limit using results like in the figure above. If the limit were set such that any location which is estimated to have 30 or more shockwaves of length 10 requires lane-change prohibitions, two small regions would be identified for consideration by Figure 26. Note that this is intended merely as an example of how a limit could be imposed. Further discussion of this will be made at the conclusion of the paper.

### 6.3 Assessment of I-35W in Minneapolis

The entire methodology presented herein was used to examine the I-35W northbound corridor. Starting from the fork where I-35 splits to I-35W/I-35E in Burnsville, MN, all detector stations which include a HOT lane detector were retrieved. The HOT corridor extends to near the I-35W/I-94 commons in downtown Minneapolis. Figure 27 shows a map of the region. From those stations, the HOT lane and adjacent general purpose lanes were identified, along with their calibrated field lengths which were used for estimating speeds from the measured volume and occupancy data. A full list of the detectors extracted from the corridor is given in Table 5.

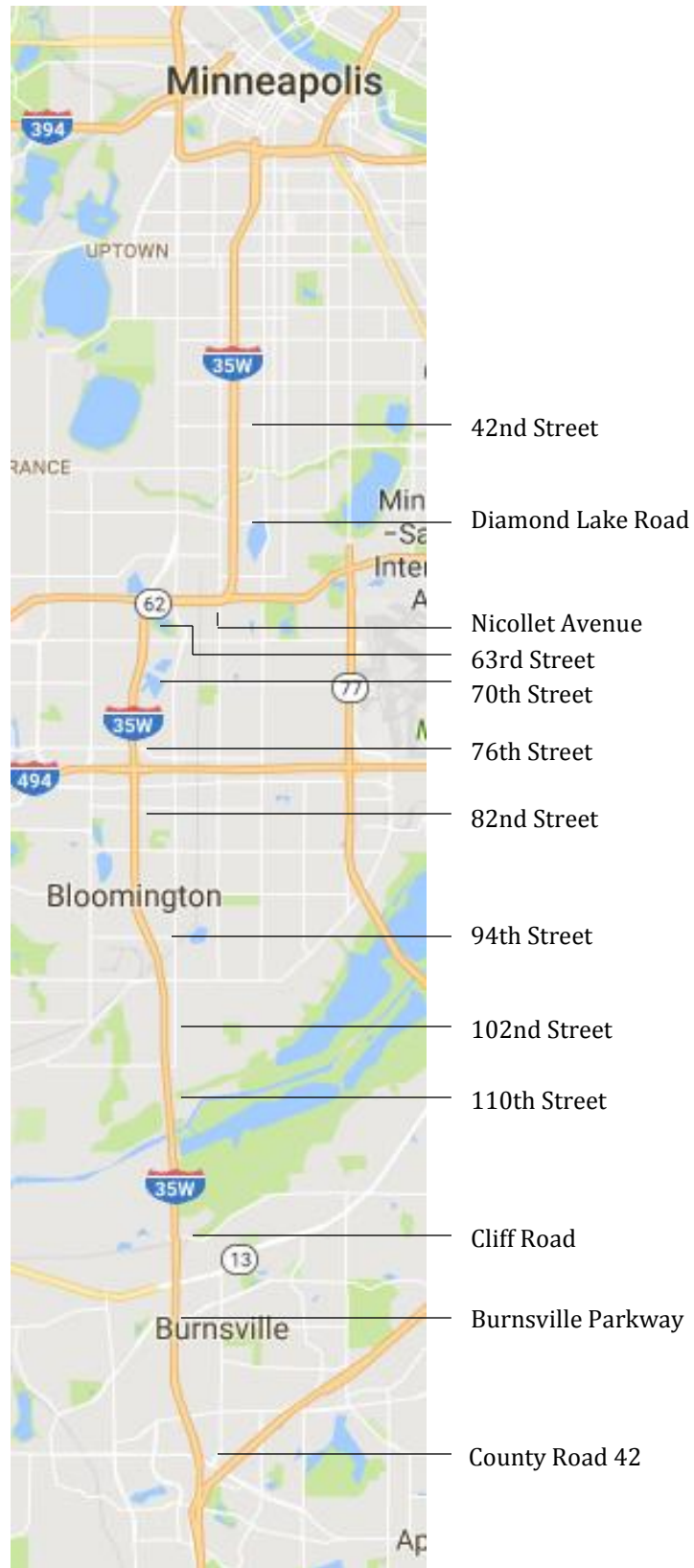


Figure 27. Map of I-35W test corridor.

Table 5. Detector information for a portion of I-35W northbound in Minneapolis.

Location	HOT Lane		Adjacent GP Lane	
	Detector ID	Field Length	Detector ID	Field Length
<i>Ordered South to North – Upstream to Downstream</i>				
County Road 42	7040	25.0	360	27.3
Timberland Drive	7042	26.4	132	23.0
Burnsville Parkway	461	26.0	259	29.9
Minnesota Highway 13	480	20.0	261	33.0
Cliff Road	500	27.2	265	31.5
113th Street	496	27.4	495	31.7
110th Street	525	27.5	267	32.0
106th Street	533	26.5	270	30.0
102nd Street	541	26.0	272	27.6
98th Street	545	26.3	274	27.5
94th Street	577	26.0	276	26.0
88th Street	579	26.0	278	28.0
85th Street	591	22.6	280	21.0
82nd Street	729	27.4	282	28.5
I-494 Interchange	3930	26.8	1177	27.0
76th Street	3933	26.0	3932	28.0
73rd Street	3934	23.0	288	27.7
70th Street	3935	23.4	290	25.5
66th Street	3938	23.8	292	29.0
63rd Street	5904	22.0	294	24.4
Lyndale Avenue	297	21.0	296	24.6
Nicollet Avenue	5923	19.6	5922	23.0
60th Street	5935	22.6	5934	25.5
Diamond Lake Road	5942	24.0	5941	24.5
46th Street	5969	22.0	5968	25.0
42nd Street	6791	24.0	318	24.5

These locations were examined during the fall of 2015, including September 1st through November 30th. Weekend dates were excluded, and both full day and peak period only data were collected. The calibrated characteristic distributions with 1000 shockwaves per speed-density condition presented in previous sections were generated. Combining these two data sets, comprehensive shockwave distributions were assembled for each location to create a corridor assessment of shockwave behavior. The resulting figure is shown below (and is the same as previously indicated).



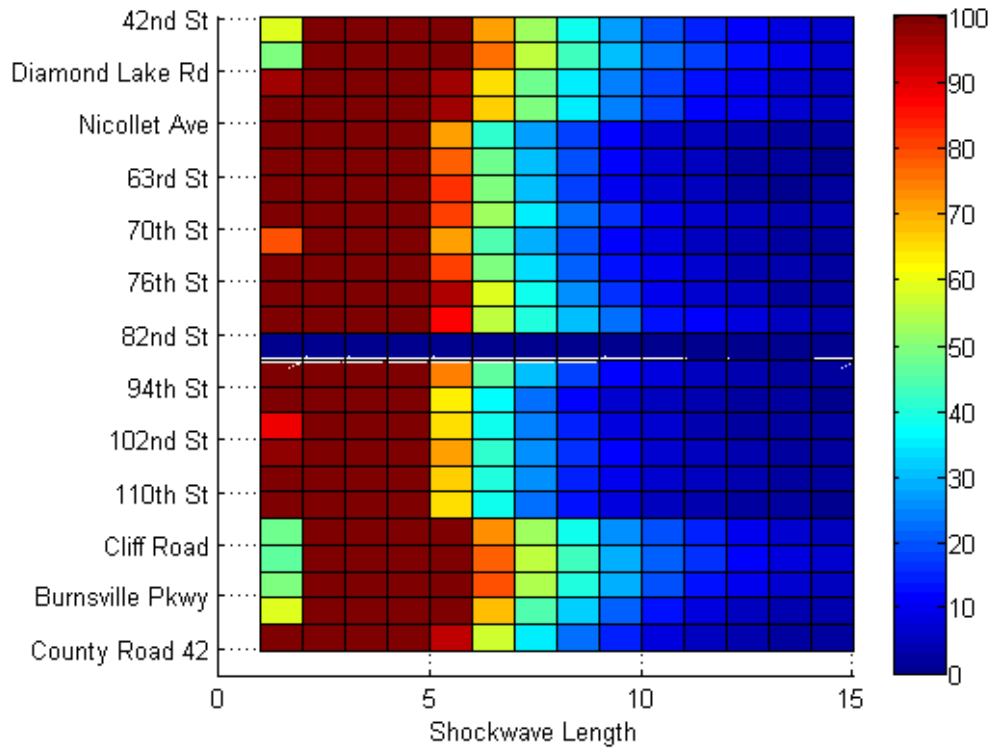


Figure 28. Comprehensive shockwave distribution using full day data.

As was previously noted, two major locations stand out as possible areas of concern for shockwave behavior: Burnsville Parkway through Cliff Road, which includes the interchange with Highway 13; and Diamond Lake Road up to 42nd Street, which includes the 46th Street bus station. In each of these segments, the relative prevalence of long shockwaves is much higher than across the rest of the corridor. Examining only the peak period data, a similar figure can be shown (Figure 29).

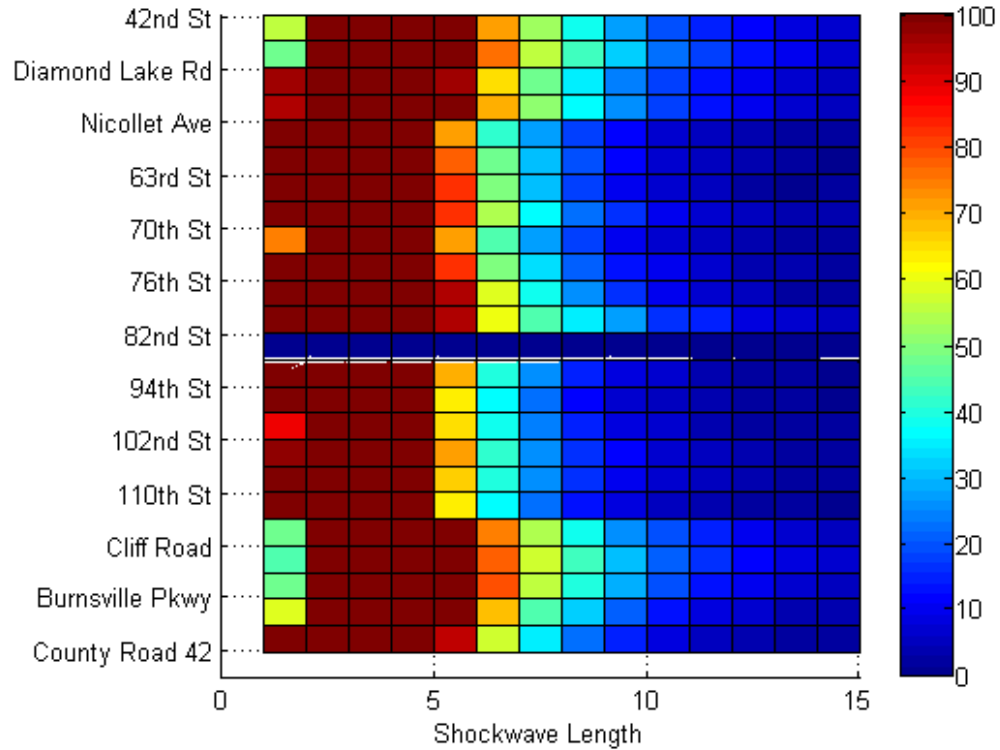


Figure 29. Comprehensive shockwave distribution using peak period only data.

Only minor differences can be seen between Figure 28 and Figure 29. In the peak-only data set, some locations shift slightly toward higher shockwaves, but the differences are negligible. This is reasonable given the findings regarding the historical data in Chapter 5. However, the percentages which fall into the four major regions across speed and density reveal an important difference. Figure 30 below shows the prevalence of data across each region when considering data across the entire day, while Figure 31 shows the prevalence of each region when only the peak periods are considered.

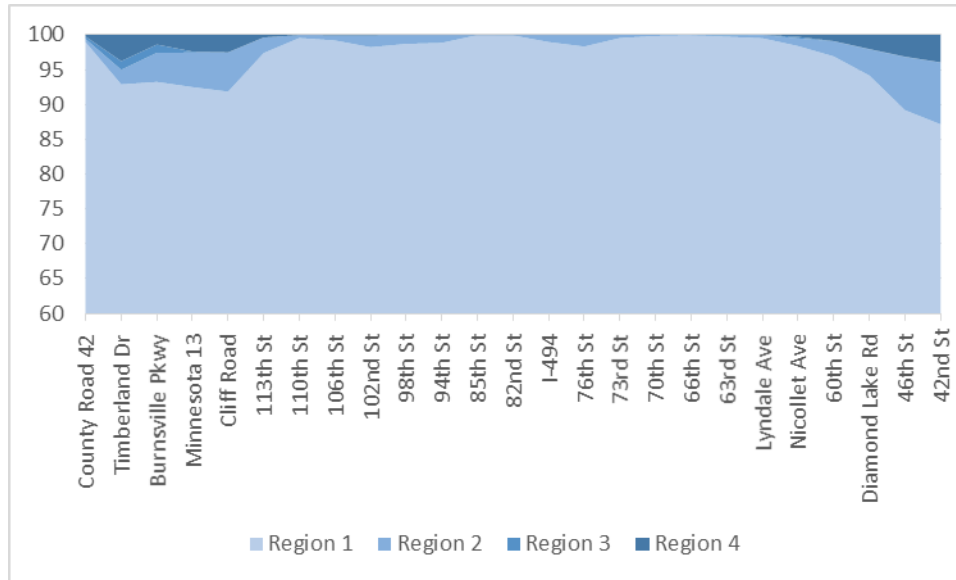


Figure 30. Proportion of speed-density regions for full day data.

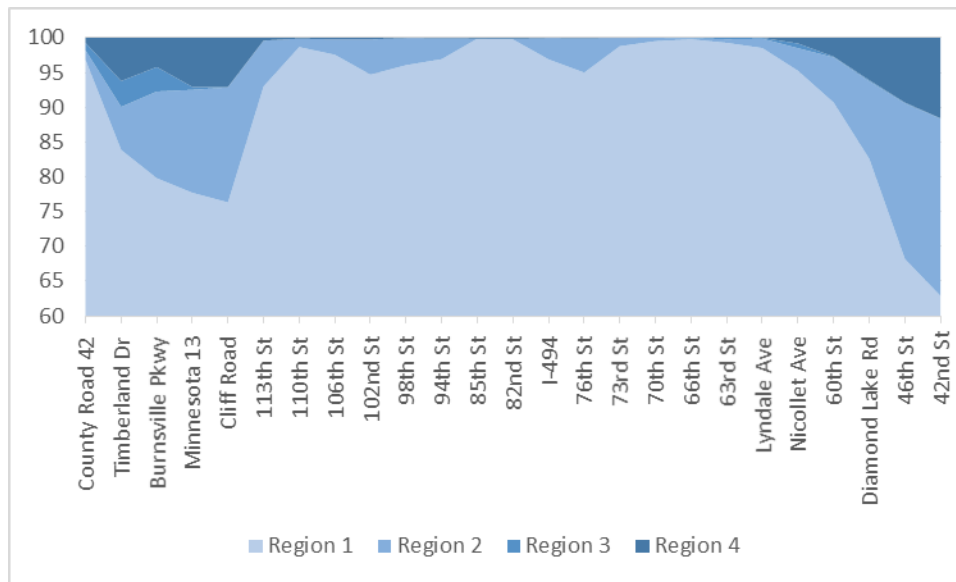


Figure 31. Proportion of speed-density regions for peak period only data.

Recalling that Region 2 indicates the range of conditions which fall under the characteristic distributions, the peak period only data reveals that certain locations make significant use of the HOT lane. These are, unsurprisingly, also the locations which have the most concern with regard to shockwaves: Burnsville parkway through Cliff Road, and

Diamond Lake Road up to 42nd Street. The region between Burnsville Parkway and Cliff Road spends roughly 12 to 15 percent of peak hour within the characteristic distribution range, while the far northern edge of the corridor at 46th and 42nd street gets up into the 20 percent range.

Also of note, the area upstream of Highway 13 has a non-trivial wedge representing Region 3 (the potentially most dangerous speed-density conditions). At both Timberland Drive and Burnsville Parkway, 3.5 to 4 percent of peak times have stopped traffic across the general purpose lanes while the HOT continues to operate at pre-congestion densities. This fits with anecdotal accounts of the corridor and data collected by Stanitsas which focused on the region around Highway 13 as a particular segment of concern.

Finally, both ends of the corridor do fall into congested conditions on the HOT for significant periods of time. This suggests that presence of major bottlenecks which even the tolling mechanism cannot resolve sufficiently. Again, this fits well with anecdotal understanding of the corridor.

Moving beyond the base-condition data described above, this methodology allows us to look toward the future operating conditions on the corridor. Using the increase scenario data developed in Chapter 5, similar figures as above were created to examine both shockwave length and region-by-region ratios within the data. Figure 32 shows the comprehensive shockwave distributions for both full-day data and peak-only data sets for each of the increase scenarios: 50% increase in density over base, 75% increase, and 100% increase.

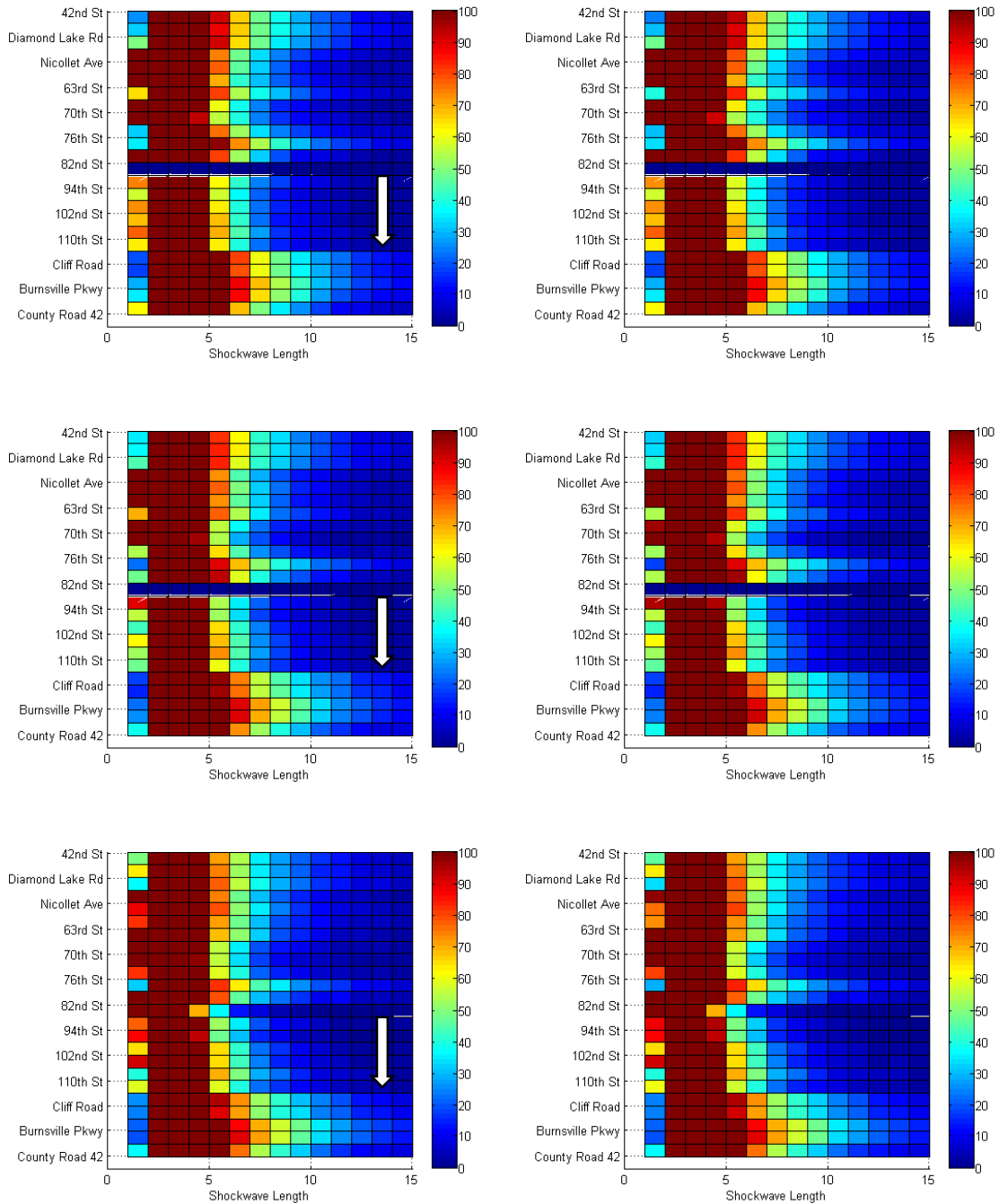


Figure 32. Comprehensive shockwave distributions for 50% increase (top), 75% increase (middle), and 100% increase (bottom) scenarios, using full day (left) or peak period only (right) data. Note slight increase in lighter blues (greater number) of long shockwaves in higher increase scenarios as indicated by inset arrows.

As can be seen in the figure, very little difference exists between the distributions using all day data and peak period only. Characteristic distribution range speed-density

combinations essentially only occur during peak period. Moving through the increase scenarios, incremental changes in the average length of shockwaves can be seen, especially around Burnsville Parkway. Interestingly, in the 100% increase scenario, the corridor develops sufficient density on the HOT and low enough speed on the adjacent general purpose lane for the characteristic distribution range to contain data at 85th Street.

Looking at the relative prevalence of the various speed-density regions, Figure 33 shows the ratios for the 50% increase scenario, Figure 34 the results for 75% increase, and finally Figure 35 shows the results for a 100% increase in density on the HOT over existing conditions.

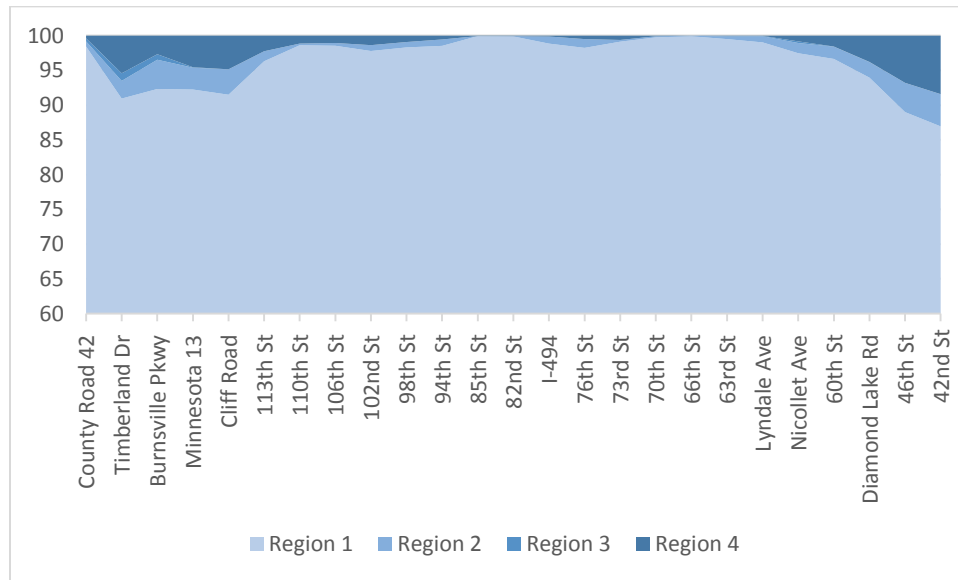


Figure 33. Proportion of speed-density regions for full day data under 50% increase scenario.

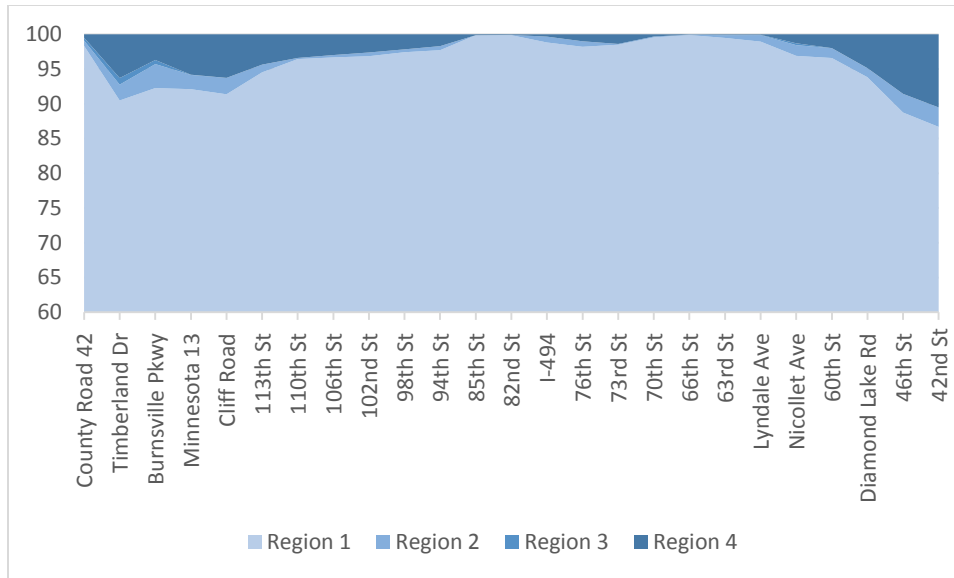


Figure 34. Proportion of speed-density regions for full day data under 75% increase scenario.

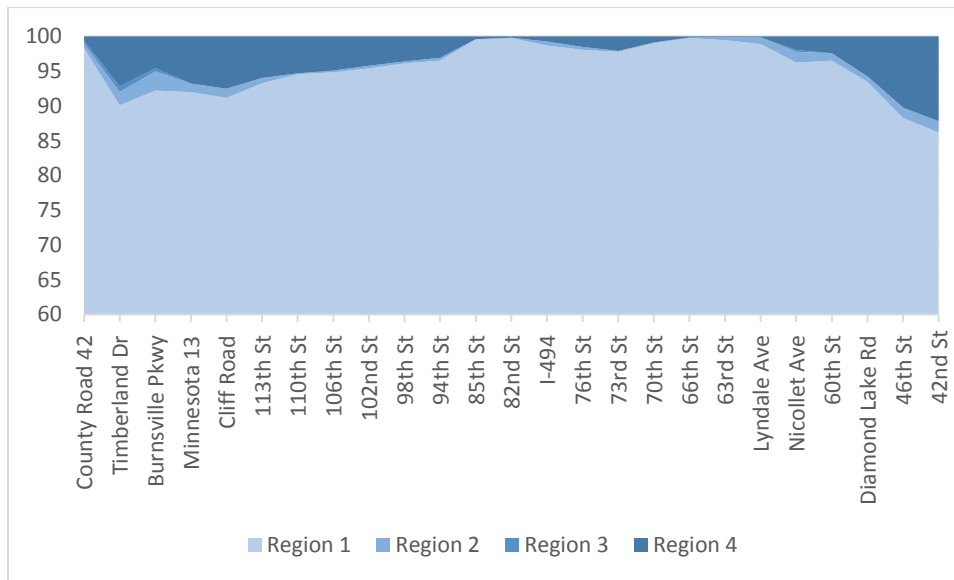


Figure 35. Proportion of speed-density regions for full day data under 100% increase scenario.

Examining the figures, it becomes clear that increasing overall density on the HOT just leads to congestion. The data show that, averaging across the entire corridor, the amount of time spent in Region 2 falls from just over 2 percent in the base condition to 0.77 percent, while Region 4 increases from 0.86 percent to 3.7 percent. If only peak period is considered, the overall pattern is similar: Region 2 falls from above 6% of data to under

just over 2%, while congested conditions on the HOT rise from near 2.3 percent to 10.5%.

These are all summarized in Table 6.

Table 6. Speed-Density region percentages by test scenario.

Scenario	% Region 1	% Region 2	% Region 3	% Region 4
Base -- All Day	96.9	2.09	0.14	0.86
+50% -- All Day	96.5	1.49	0.12	1.92
+75% -- All Day	96.0	1.08	0.10	2.82
+100% -- All Day	95.4	0.77	0.08	3.70
Base -- Peak Only	91.1	6.15	0.42	2.29
+50% -- Peak Only	90.0	4.34	0.34	5.33
+75% -- Peak Only	88.7	3.12	0.28	7.93
+100% -- Peak Only	87.1	2.19	0.23	10.50

Also in the table are the results when considering only the peak period. As expected, the percentages are greater in magnitude than within the all-day data sets but the overall trends are similar. Figure 36, Figure 37, and Figure 38 below show the values for peak period only.

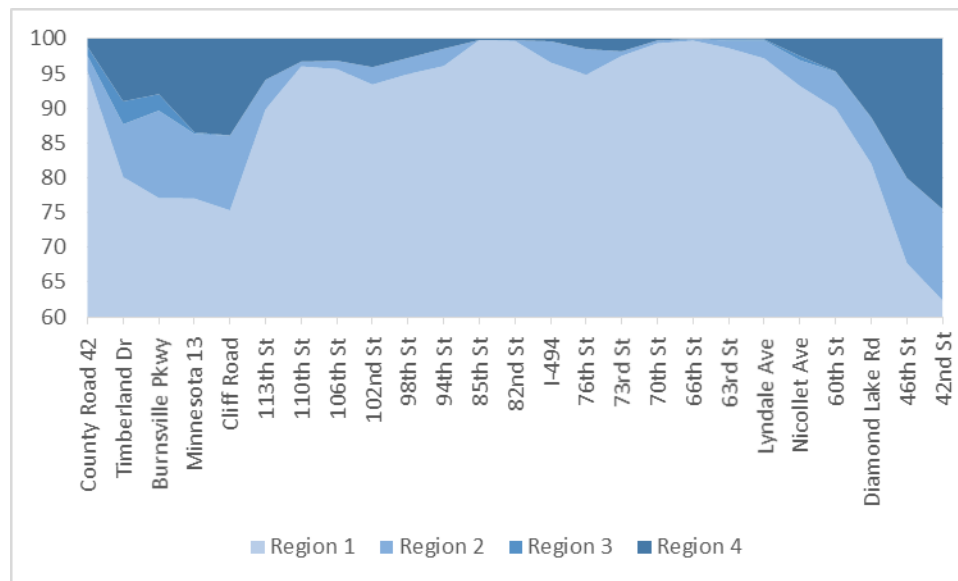


Figure 36. Proportion of speed-density regions for peak period data under 50% increase scenario.



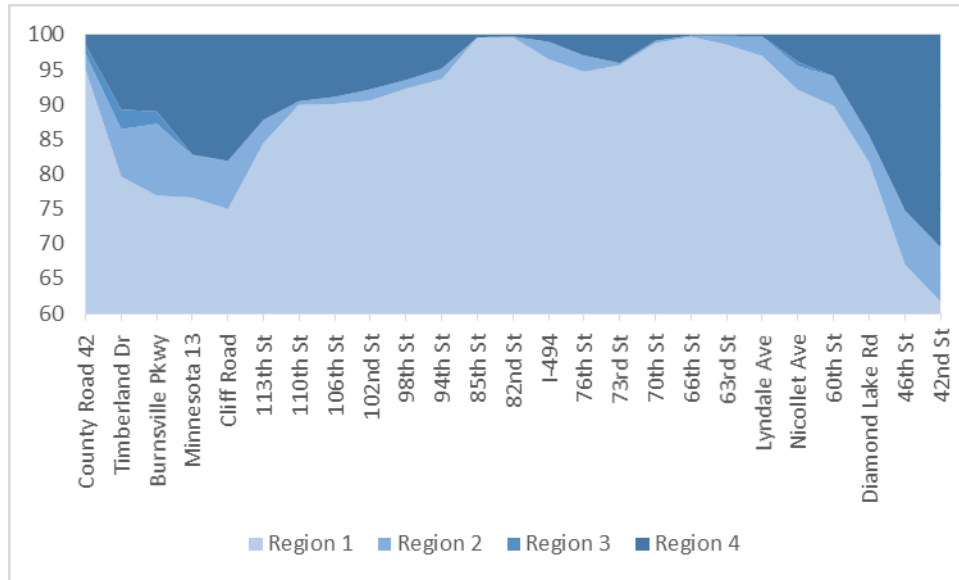


Figure 37. Proportion of speed-density regions for peak period data under 75% increase scenario.

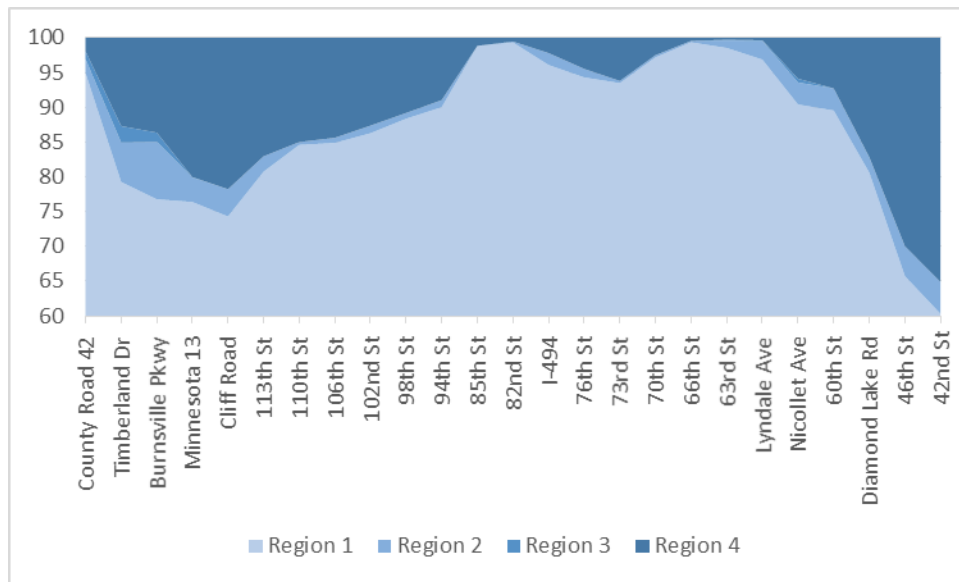


Figure 38. Proportion of speed-density regions for peak period data under 100% increase scenario.

By examining the figures above, especially the final figure showing the 100% increase scenario, we can see that the HOT lane has significant usage at the two locations of concern which we have already found (Burnsville Parkway/Highway 13 area, and 46th Street and north). However, we also see that the HOT has notable usage north of the Highway 13/Cliff Road bottleneck up through 85th street. Efforts to increase HOT

utilization through changes in the tolling mechanism or simply general increase in use due to growth in traffic on the corridor will push the entire southern half of the corridor toward significant periods of breakdown. Interestingly, even with double the density on the HOT, the I-494 interchanges does not become as significantly broken down as the rest of the corridor.

## Chapter 7 - Conclusion

The methodology presented in this paper provides a tool for traffic managers and planners to examine the conditions within an existing or prospective corridor and the distribution of shockwave lengths which are expected. From the distribution of shockwave lengths, decisions can be made regarding access restriction on the HOT lane to ensure that drivers do not attempt to make lane changes at locations prone to dangerous conditions. This tool provides support for the managers and planners by aggregating the entire behavior of the HOT lane within the corridor into a framework for simplified consideration.

This methodology is a dramatic improvement and expansion of previous efforts. Stream generation was reworked to ensure a good mix of target stream densities and speeds are created, and to include perturbation and simulation in order to ensure that the vehicle streams used for simulation are realistic. Shockwave simulations were greatly improved through the inclusion of a complete car following model and additional parameters and behaviors to capture the ability of drivers to observe beyond their immediate leader. The entire Monte Carlo sampling framework was also extended throughout a corridor by the inclusion of an assessment of historical data. Ultimately, the results produced by this methodology are more robust than previous approaches.

There are still several areas in which improvements could be made. At the core, this methodology is based on the data collected along the I-35W and I-394 HOT lanes. The extent of that data limited the scope of calibration and validation for the tool. Notably, no data was collected while the HOT was at densities approaching breakdown (33 to 42 vpm). Within that scope, it is possible that driver behavior changes significantly since gaps are much smaller. Regarding those underlying behaviors, two components were incorporated

into the model through calibration in order to produce satisfactory results: a scaling sensitivity coefficient on the GM car following model, and a look ahead mechanism which also scales with density. In both cases, linear relationships between density and the parameter were introduced to shift driver behavior as density increases. However, lacking calibration data or specific measurements of how drivers perform (especially with regard to look ahead), these mechanisms are only estimations based on engineering judgement of reasonable behavior.

Regarding the car following model, although many different calibrations were attempted, it is possible that a more accurate set of calibration values exists. Again, a more robust dataset of real-world shockwave measurements would aid in producing a well-fitting car following model. Other car following models entirely may also fit the situation more accurately. This methodology fixed upon the GM model due to the simple inputs of position and speed and the relatively flexible framework of its calibration parameters. Other car following models were not fully considered and could replace the GM model within the methodology. Fortunately, the development of this tool proceeded in such a way that the car following model is isolated within the model, allowing for relatively straightforward replacement.

When combining the resulting characteristic shockwave distributions with historical data to produce comprehensive shockwave distributions, two important assumptions are made regarding the corridor: that the lane change frequency between the GP and HOT is constant over time, and is also evenly distributed across the corridor. Both of these assumptions raise crucial issues regarding the management of the HOT, but the mechanisms necessary to resolve them are far from trivial. This methodology makes these

assumptions to provide a simplified view of a corridor's behavior and allow traffic managers to gain insight into potential safety hazards without requiring the construction and calibration of a micro-simulation model. In the case that information regarding these two assumptions is available, additional weighting could be introduced to this methodology to improve the resulting assessment.

Essentially, these additional weightings would allow the arbitrary “number of shockwaves” value on the y-axis of the comprehensive shockwave distributions, which currently only provides relative information along the corridor, to provide a meaningful measure of the number of travelers exposed to shockwaves of varying length. This would make the entire procedure more immediately understandable and also allow for more direct performance targets to be established. A critical number of travelers exposed to shockwaves of a target length (or longer shockwaves) could be used to impose lane change prohibitions for a segment of a corridor, for example.

Even without making the step to determine exposure, the relative distributions throughout a corridor provide interesting operational information in addition to safety understanding. The existing HOT corridor on I-35W includes a set of zones where pricing changes. Ideally, these would be placed and controlled in such a way that the entire HOT corridor would experience even and strong usage in order to alleviate congestion throughout. The comprehensive shockwave distribution for the existing state of the corridor indicates that three regions appear to operate differently. Around the south and north ends of the corridor, more significant congestion is present and the HOT experiences more and longer shockwaves. In between a large space exists with shorter shockwaves and lower use on the HOT. This may indicate that the pricing structure along the corridor

should be changed to allow for a more nuanced tolling approach in order to make use of capacity in this region. Other corridors could similarly be analyzed and have trends in usage compared with tolling mechanisms and plaza layouts.

Finally, this paper explores the possibility of increased density scenarios with regard to the HOT. Those scenarios were constructed by scaling up the density on the HOT at all times of day while leaving the activity on the general purpose lanes unaltered. While interesting, these increase scenarios are not realistic in the sense that the HOT and GP lanes both change as demand across the corridor increases. A more robust mechanism for estimating future conditions would lead to more realistic estimates of future comprehensive distributions. Rather than the dramatic increase in congested HOT which was developed with the increase scenarios in the previous chapter, a larger component of characteristic distribution-range conditions would be expected given that the tolling mechanism on the HOT works to maintain operations on the lane. If demand across the corridor increases, the tolling mechanism pushes back to keep the HOT lane functioning, prolonging pre-congestion conditions as much as possible.

## References

1. Light, T. *High Occupancy Toll Lane Performance Under Alternative Pricing Policies*. Journal of the Transportation Research Forum, Vol. 51, No. 2. (2012)  
<<http://ageconsearch.umn.edu/bitstream/207318/2/2911-5636-1-PB.pdf>>
2. Zhang, G., X. Ma, and Y. Wang. *Self-Adaptive Tolling Strategy for Enhanced High-Occupancy Toll Lane Operations*. IEEE Transactions on Intelligent Transportation Systems, Vol. 15, No. 1. (2014)  
<<http://ieeexplore.ieee.org.ezp3.lib.umn.edu/stamp/stamp.jsp?arnumber=6606899>>
3. Lou, Y., Y. Yin, and J. Laval. *Optimal Dynamic Pricing Strategies for High-Occupancy/Toll Lanes*. Transportation Research Part C: Emerging Technologies, Vol. 19, Iss. 1. (2011)  
<[http://ac.els-cdn.com.ezp3.lib.umn.edu/S0968090X10000343/1-s2.0-S0968090X10000343-main.pdf?\\_tid=7c3e923c-7767-11e6-88a2-00000aab0f27&acdnat=1473519883\\_fd3929914930c34e8f17cdb43eaf50a2](http://ac.els-cdn.com.ezp3.lib.umn.edu/S0968090X10000343/1-s2.0-S0968090X10000343-main.pdf?_tid=7c3e923c-7767-11e6-88a2-00000aab0f27&acdnat=1473519883_fd3929914930c34e8f17cdb43eaf50a2)>
4. Jang, K., K. Chung, and H. Yeo. *A Dynamic Pricing Strategy for High Occupancy Toll Lanes*. Transportation Research Part A: Policy and Practice, Vol. 67. (2014)  
<[http://ac.els-cdn.com.ezp3.lib.umn.edu/S0965856414001232/1-s2.0-S0965856414001232-main.pdf?\\_tid=8638d6bc-7767-11e6-9dfc-00000aab0f26&acdnat=1473519899\\_3851545245213ce2088eb14f0119f8f9](http://ac.els-cdn.com.ezp3.lib.umn.edu/S0965856414001232/1-s2.0-S0965856414001232-main.pdf?_tid=8638d6bc-7767-11e6-9dfc-00000aab0f26&acdnat=1473519899_3851545245213ce2088eb14f0119f8f9)>
5. Jang, K., M. Song, K. Choi, and D. Kim. *A Bi-Level Framework for Pricing of High-Occupancy Toll Lanes*. Transport, Vol. 29, Iss. 3. (2014)  
<<http://www.tandfonline.com/doi/abs/10.3846/16484142.2014.952248>>
6. Federal Highway Administration. *Investigating Congestion and Solutions: Experiments on Congestion Conditions and Pricing Initiatives*. The Exploratory Advanced Research Program Fact Sheet, FHWA-HRT-10-061. (2010)  
<<http://permanent.access.gpo.gov/gpo8159/10061.pdf>>
7. Li, J. *Explaining High-Occupancy-Toll Lane Use*. Transportation Research Part D: Transport and Environment, Vol. 6, Iss. 1. (2001)  
<[http://ac.els-cdn.com.ezp3.lib.umn.edu/S1361920900000134/1-s2.0-S1361920900000134-main.pdf?\\_tid=3f1567ac-776a-11e6-a0ca-00000aab0f6b&acdnat=1473521069\\_4359883ce330002e0958a46afce24b66](http://ac.els-cdn.com.ezp3.lib.umn.edu/S1361920900000134/1-s2.0-S1361920900000134-main.pdf?_tid=3f1567ac-776a-11e6-a0ca-00000aab0f6b&acdnat=1473521069_4359883ce330002e0958a46afce24b66)>
8. Lee, K., A. Hobeika, H. Zhang, and H. Jung. *Travelers' Response to Value Pricing: Application of Departure Time Choices to TRANSIMS*. Journal of Transportation Engineering, Vol. 136, Iss. 9. (2010)  
<<http://ascelibrary.org.ezp3.lib.umn.edu/doi/pdf/10.1061/%28ASCE%29TE.1943-5436.0000139>>

9. Boyles, S., L. Gardner, and H. Bar-Gera. *Incorporating Departure Time Choice into High Occupancy/Toll (HOT) Algorithm Evaluation*. Transportation Research Procedia, Vol. 9. (2015)  
<[http://ac.els-cdn.com.ezp3.lib.umn.edu/S2352146515001660/1-s2.0-S2352146515001660-main.pdf?\\_tid=53b2cd1c-776a-11e6-b4fc-00000aab0f27&acdnat=1473521103\\_e886a396875cd0a62cb18b2d8dd5071d](http://ac.els-cdn.com.ezp3.lib.umn.edu/S2352146515001660/1-s2.0-S2352146515001660-main.pdf?_tid=53b2cd1c-776a-11e6-b4fc-00000aab0f27&acdnat=1473521103_e886a396875cd0a62cb18b2d8dd5071d)>
10. Zhang, G., S. Yan, and Y. Wang. *Simulation-Based Investigation on High-Occupancy Toll Lane Operations for Washington State Route 167*. Journal of Transportation Engineering, Vol. 135, Iss. 10. (2009)  
<<http://ascelibrary.org.ezp3.lib.umn.edu/doi/pdf/10.1061/%28ASCE%290733-947X%282009%29135%3A10%28677%29>>
11. Chung, C., and W. Recker. *Evaluation of Operational Effects of Joint Managed Lane Policies*. Journal of Transportation Engineering, Vol. 138, Iss. 7. (2012)  
<<http://ascelibrary.org.ezp3.lib.umn.edu/doi/pdf/10.1061/%28ASCE%29TE.1943-5436.0000385>>
12. Fielding, G., and D. Klein. *High Occupancy/Toll Lanes: Phasing in Congestion Pricing a Lane at a Time*. Reason Foundation: Policy Study No. 170. (1993)  
<<http://reason.org/files/22b593c21e642143157e65dc5223ce9a.pdf>>
13. Washington State Department of Transportation. *HOT Lane Buffer and Mid-Point Access: Design Review Report*. (2006)  
<<http://www.wsdot.wa.gov/research/reports/fullreports/651.1.pdf>>
14. Texas Department of Transportation. *Roadway Design Manual*. (2014)  
<<http://onlinemanuals.txdot.gov/txdotmanuals/rdw/rdw.pdf>>
15. Federal Highway Administration. *Priced Managed Lane Guide*. FHWA-HOP-13-007. (2012)  
<<http://ops.fhwa.dot.gov/publications/fhwahop13007/fhwahop13007.pdf>>
16. Florida Department of Transportation. *Express Lanes Handbook*. (2015)  
<<http://www.floridaexpresslanes.com/wp-content/uploads/2015/08/FDOT-Express-Lanes-Handbook.pdf>>
17. Nevada Department of Transportation. *Managed Lanes and Ramp Metering Manual Part 3: Design Manual*. (2013)  
<[https://www.nevadadot.com/uploadedFiles/NDOT/About\\_NDOT/NDOT\\_Divisions/Planning/Safety\\_Engineering/Design%20Manual.pdf](https://www.nevadadot.com/uploadedFiles/NDOT/About_NDOT/NDOT_Divisions/Planning/Safety_Engineering/Design%20Manual.pdf)>
18. Florida Department of Transportation. *Crash Prediction Method for Freeway Facilities with High Occupancy Vehicle (HOV) and High Occupancy Toll (HOT) Lanes*. (2015)



- <[http://www.dot.state.fl.us/research-center/completed\\_Proj/Summary\\_RD/FDOT-BDV32-977-04-rpt.pdf](http://www.dot.state.fl.us/research-center/completed_Proj/Summary_RD/FDOT-BDV32-977-04-rpt.pdf)>
19. Chanlder, R., R. Herman, and E. Montroll. *Traffic Dynamics: Studies in Car Following*. Operations Research, Vol. 6, No. 2. (1958)  
<<http://www.mathstat.dal.ca/~iron/math4190/Papers/traffic.pdf>>
  20. Benehokal, R., A. Kaja-Mohideen, and M. Chitturi. *Methodology for Estimating Operating Speed and Capacity in Work Zones*. Transportation Research Record, Volume 1883. (2014)  
<<http://trrjournalonline.trb.org/doi/pdf/10.3141/1883-12>>
  21. National Conference of State Legislatures. *Toll Facilities in the United States*. (2012)  
<[http://www.ncsl.org/research/transportation/toll-facilities-in-the-united-states.aspx#Map\\_1\\_Toll\\_Facilities](http://www.ncsl.org/research/transportation/toll-facilities-in-the-united-states.aspx#Map_1_Toll_Facilities)>
  22. Stanitsas, P. *A New Design Approach for High Occupancy Toll Lanes*. University of Minnesota Digital Conservancy. (2013)  
<<http://conservancy.umn.edu/handle/11299/160303>>
  23. Federal Highway Administration. *Managed Lanes: A Primer*. FHWA-HOP-05-031. (2005)  
<[http://ops.fhwa.dot.gov/publications/managelanes\\_primer/managed\\_lanes\\_primer.pdf](http://ops.fhwa.dot.gov/publications/managelanes_primer/managed_lanes_primer.pdf)>
  24. Federal Highway Administration. *Congestion Pricing Projects Open to Traffic in the United States as of January 2012*. (2012)  
<[http://ops.fhwa.dot.gov/freewaymgmt/managed\\_lanes/congest\\_proj\\_jan12.htm](http://ops.fhwa.dot.gov/freewaymgmt/managed_lanes/congest_proj_jan12.htm)>
  25. Technical Committee on Public Transportation Facilities Design, AASHTO. *Guide for High-Occupancy Vehicle (HOV) Facilities*. (2004)  
<<https://bookstore.transportation.org/imageview.aspx?id=315&DB=3>>